J. metamorphic Geol., 2004, **22,** 607–627 doi:10.1111/j.1525-1314.2004.00537.x

The regional significance of Cretaceous magmatism and metamorphism in Fiordland, New Zealand, from U–Pb zircon geochronology

J. A. HOLLIS[1], G. L. CLARKE[1], K. A. KLEPEIS[2], N. R. DACZKO[1,3] AND T. R. IRELAND[4]
[1]*School of Geosciences, University of Sydney, NSW 2006, Australia (jho@geus.dk)*
[2]*Department of Geology, The University of Vermont, Burlington, VT 05405, USA*
[3]*Department of Earth and Planetary Sciences, Macquarie University, NSW 2109, Australia*
[4]*Research School of Earth Sciences, Australian National University, Canberra ACT 0200, Australia*

ABSTRACT The western Fiordland Orthogneiss (WFO) is an extensive composite metagabbroic to dioritic arc batholith that was emplaced at *c.* 20–25 km crustal depth into Palaeozoic and Mesozoic gneiss during collision and accretion of the arc with the Mesozoic Pacific Gondwana margin. Sensitive high-resolution ion microprobe U–Pb zircon data from central and northern Fiordland indicate that WFO plutons were emplaced throughout the early Cretaceous (123.6 ± 3.0, 121.8 ± 1.7, 120.0 ± 2.6 and 115.6 ± 2.4 Ma). Emplacement of the WFO synchronous with regional deformation and collisional-style orogenesis is illustrated by (i) coeval ages of a post-D1 dyke (123.6 ± 3.0 Ma) and its host pluton (121.8 ± 1.7 Ma) at Mt Daniel and (ii) coeval ages of pluton emplacement and metamorphism/deformation of proximal paragneiss in George and Doubtful Sounds. The coincidence emplacement and metamorphic ages indicate that the WFO was regionally significant as a heat source for amphibolite to granulite facies metamorphism. The age spectra of detrital zircon populations were characterized for four paragneiss samples. A paragneiss from Doubtful Sound shows a similar age spectrum to other central Fiordland and Westland paragneiss and SE Australian Ordovician sedimentary rocks, with age peaks at 600–500 and 1100–900 Ma, a smaller peak at *c.* 1400 Ma, and a minor Archean component. Similarly, one sample of the George Sound paragneiss has a significant Palaeozoic to Archean age spectrum, however zircon populations from the George Sound paragneiss are dominated by Permo-Triassic components and thus are markedly different from any of those previously studied in Fiordland.

Key words: Doubtful Sound; Fiordland; George Sound paragneiss; sensitive high-resolution ion microprobe; western Fiordland Orthogneiss; zircon geochronology.

INTRODUCTION

The early Cretaceous western Fiordland Orthogneiss (WFO) is an extensive granulite facies composite batholith that is exposed along the length of the Fiordland Block in south-west New Zealand (*c.* 120 × 30 km; Fig. 1). It comprises gabbroic to dioritic orthogneiss emplaced into Palaeozoic ortho- and paragneiss and Mesozoic orthogneiss thought to represent the rifted and tectonically dismembered remnants of the Palaeo-Pacific Gondwana margin. During the Mesozoic, the Pacific Gondwana margin experienced rapid changes in tectonic environments involving the transition from outboard arc magmatism to arc-continent collision to continental rifting leading to the opening of the Tasman Sea (Mattinson *et al.*, 1986; McCulloch *et al.*, 1987; Bradshaw, 1989a,b; Kimbrough *et al.*, 1994; Weaver *et al.*, 1994; Muir *et al.*, 1998; Wandres *et al.*, 1998; Clarke *et al.*, 2000; Daczko *et al.*, 2001a,b; Hollis *et al.*, 2003). The emplacement of WFO plutons reflects the final stages of arc magmatism along the long-lived palaeo-Pacific convergent margin. Therefore examination of the WFO, its timing and setting of emplacement, metamorphism related to the WFO thermal pulse, and structural constraints on its evolution have the potential for advancing our knowledge of the crustal response to changing tectonic setting in an evolving plate boundary zone in general and evolution of the Mesozoic Pacific Gondwana margin in particular.

Owing to differing interpretations of the timing of development of key metamorphic assemblages, and the tectonic significance and timing of high-grade deformation features, divergent hypotheses have been proposed for the tectonic setting of emplacement of the WFO. These hypotheses include magmatism during arc-continent collision (Mattinson *et al.*, 1986; McCulloch *et al.*, 1987; Bradshaw, 1989b; Clarke

Present address: Julie A. Hollis, Department of Geological Mapping, Geological Survey of Denmark and Greenland, Øster Voldgade 10, K-1350 Copenhagen, Denmark.

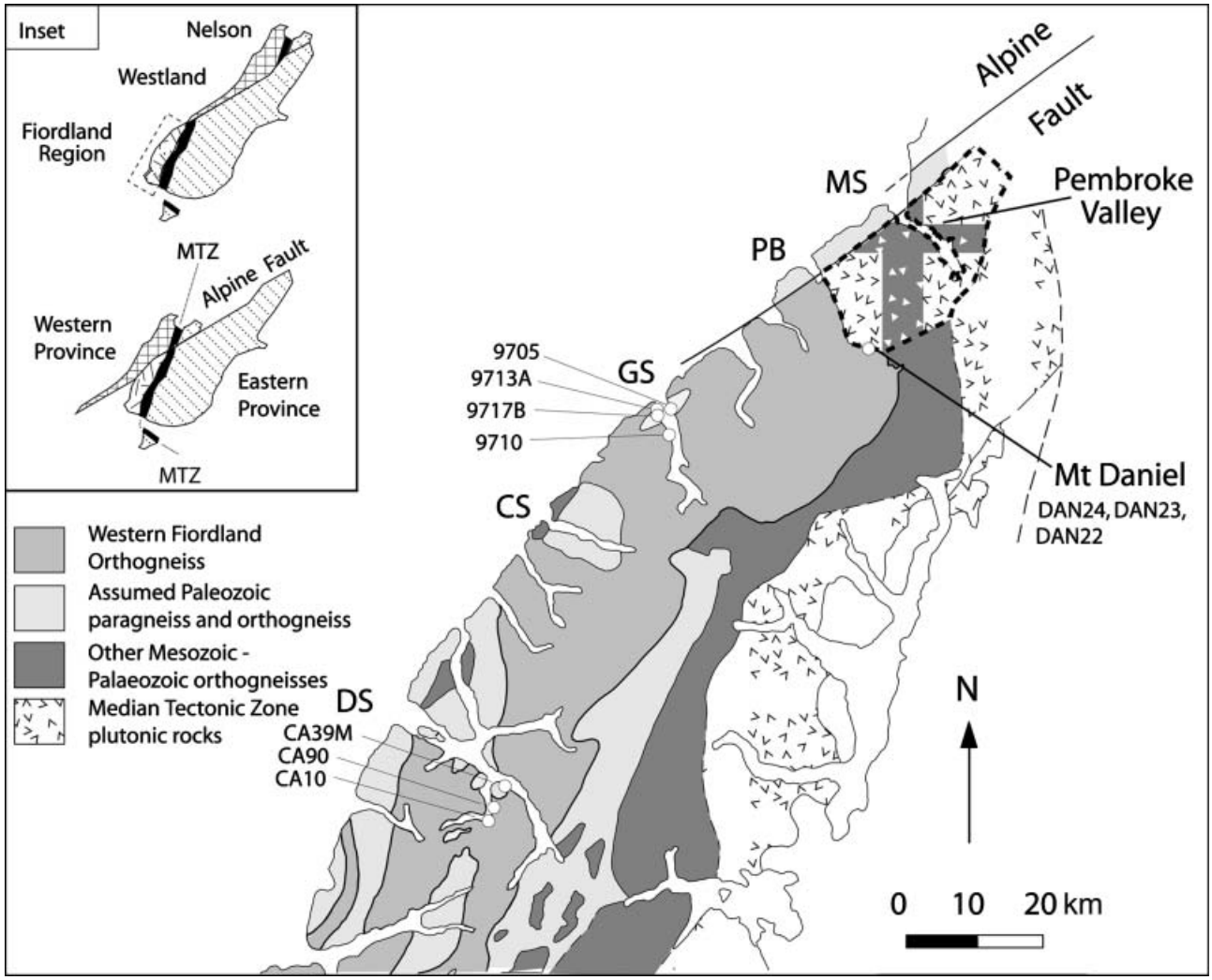

Fig. 1. Regional geology of Fiordland showing locations of samples. MS, Milford Sound; PB, Poison Bay; GS, George Sound; CS, Caswell Sound; DS, Doubtful Sound. The Arthur River Complex, the youngest recognized phase of MTZ magmatism, is shown with a dashed outline.

et al., 2000; Daczko *et al.*, 2001a,b), crustal thickening via magmatic loading of the crust (Oliver, 1990; Brown, 1996), and magmatism associated with continental rifting during the development of a metamorphic core complex (Gibson *et al.*, 1988; Gibson & Ireland, 1995). Both collisional tectonism and continental rifting have been shown to be important factors in the Cretaceous evolution of the Western Province of New Zealand. In order to understand their relationship with WFO magmatism the following three issues are seen as fundamental: (i) the timing of emplacement, deformation, and metamorphism of the WFO, (ii) the timing of development of metamorphic assemblages in central and northern Fiordland in general, and (iii) the nature of the crust into which the WFO was emplaced. In this paper these issues are addressed via a U–Pb zircon study of the WFO and para- and orthogneiss with which it shows clear intrusional relationships.

GEOLOGICAL AND GEOCHRONOLOGICAL SETTING

The South Island of New Zealand has been divided into (i) the Eastern Province, (ii) the Median Tectonic Zone (MTZ) or Median Batholith, and (iii) the Western Province (Landis & Coombs, 1967; Kimbrough *et al.*, 1993, 1994; Mortimer *et al.*, 1999). The boundaries between the provinces are largely fault-controlled, though stitching plutons indicate amalgamation of the Eastern Province and the MTZ by the late Triassic (Williams & Harper, 1978) and the MTZ and the Western Province by the early Cretaceous (*c.* 136 Ma; Hollis *et al.*, 2003). All three terranes have been disrupted and displaced by *c.* 480 km along the Tertiary Alpine Fault.

The Eastern Province comprises fault-bound Permian to early Cretaceous tectonostratigraphic terranes comprising dominantly turbiditic, volcanic, and

volcanoclastic sedimentary rocks (Fig. 1). These are dominated by the greenschist facies metasedimentary rocks of the Torlesse Supergroup, Caples Group, and the Haast Schist. Samples of the turbiditic Torlesse, and of volcanoclastic rocks of the Maitai, Murihiku, and Brook St Terranes have dominantly Permian to Triassic detrital zircon U–Pb age spectra consistent with initiation of sedimentation in the Permian (Ireland, 1992; Kimbrough *et al*., 1992; Adams *et al*., 2002).

The MTZ comprises a belt of subduction-related plutonic, volcanic and sedimentary rocks thought to have formed within a Mesozoic magmatic arc within or outboard of the Pacific Gondwana margin. Two distinct phases of magmatic activity occurred from 345 to 195 Ma and from 168 to 137 Ma (Bradshaw, 1993; Kimbrough *et al*., 1993, 1994; Muir *et al*., 1998). Rocks belonging to the late Triassic to early Cretaceous phase are volumetrically dominant and preferentially distributed in the western region of the MTZ in both Nelson and Fiordland (Kimbrough *et al*., 1994). On the basis of U–Pb geochronology and geochemical characteristics, Hollis *et al*. (2003) proposed that 136–129 Ma emplacement of the dioritic to gabbroic protoliths of the granulite facies Arthur River Complex (ARC) in Northern Fiordland represents the final stages of MTZ magmatism shortly after amalgamation of the MTZ and the Western Province and prior to the emplacement of the WFO.

Palaeozoic paragneiss and Palaeozoic and Mesozoic orthogneiss of the once contiguous Nelson/ Westland and Fiordland regions, which comprise the Western Province, represent the upper and lower sections, respectively, of Mesozoic continental Gondwana crust. The Nelson/ Westland region comprises low-grade metasedimentary rocks intruded by Carboniferous to Devonian and Cretaceous granitic rocks. Low-pressure upper amphibolite facies metamorphic rocks are associated with both phases of magmatic activity; in the Charleston Metamorphic complex Cretaceous ortho- and paragneiss are preserved, whereas both Cretaceous and Palaeozoic paragneiss are found in the Mt Victoria Range (Kimbrough & Tulloch, 1989; Ireland, 1992; White, 1994). In contrast the Western Province in Fiordland is dominated by mid to lower crustal rocks (>25 km depth).

The central Fiordland metasedimentary rocks are generally inferred to be all of Palaeozoic age, however this is based on limited geochronological data restricted to samples from the Doubtful Sound region and it is possible that there is considerable diversity in their ages and origins. U–Pb detrital zircon age spectra from these and samples from the Westland/Nelson region exhibit prominent age peaks at 600–500, 1100–1000, and 1700 Ma, and with a minor Archean component (Ireland, 1992; Wysoczanski *et al*., 1997; Ireland *et al*., 1998; Ireland & Gibson, 1998). This age spectra has been referred to as the Pacific Gondwana component and is common to Ordovician sedimentary rocks of the Lachlan Fold Belt, and paragneiss of Northern Victoria Land and Marie Byrd Land (Adams, 1987; Weaver *et al*., 1991; Cooper & Tulloch, 1992; Ireland *et al*., 1994; Fergusson & Fanning, 2002).

In the mid-Palaeozoic widespread subduction-related calc-alkaline magmatism (*c*. 420–250 Ma) occurred in the Western Province and contiguous regions including the Lachlan Fold Belt (Chappell & White, 1992; Williams *et al*., 1992), Northern Victoria Land, Marie Byrd Land (Adams, 1987; Borg *et al*., 1987; Weaver *et al*., 1991), and the New England Fold Belt (Ewart *et al*., 1992). Fiordland rocks experienced low-pressure metamorphism of paragneiss in the Doubtful Sound region at *c*. 360 Ma (cordierite $\pm$ K-feldspar-bearing; 3–5 kbar), followed by high-pressure metamorphism at *c*. 330 Ma (kyanite-grade; 5–9 kbar) with no discernible change in temperature conditions (630–680 °C cf. 580–780 °C, respectively; Ireland & Gibson, 1998). Metamorphism was probably related to emplacement of Devonian intrusive rocks such as the Karamea batholith in Westland (*c*. 375 Ma; Muir *et al*., 1996). Similar low-pressure (andalusite to sillimanite-grade) followed by high-pressure (650–700 °C, 12–13 kbar) metamorphism has been reported for the George Sound paragneiss (GSP) in northern Fiordland (Bradshaw, 1989b), although correlation with assemblages in central Fiordland has been limited until now due to lack of radiometric age data for the GSP.

The dominant expression of Cretaceous magmatism in Fiordland is the WFO, a regionally extensive gabbroic to dioritic composite batholith, now metamorphosed to amphibolite to granulite facies. It was emplaced between 126 and 119 Ma, shortly after the 136–129 Ma ARC of northern Fiordland (Bradshaw, 1985, 1989b; Mattinson *et al*., 1986; McCulloch *et al*., 1987; Hollis *et al*., 2003). In Doubtful Sound the WFO is in fault-contact with an ortho- and paragneissic sequence along the Doubtful Sound shear zone, within which both the WFO and adjacent ortho- and paragneiss show intense ductile deformation and recrystallization. In northern and central Fiordland, at George Sound, Mt Daniel and other locations in the Franklin Mountains, intrusive relationships and xenoliths of paragneiss, granitoids and orthogneiss within the WFO have been described (Bradshaw, 1989b; Bradshaw & Kimbrough, 1991). In George Sound the WFO shows clear intrusional relationships with the GSP, including the development of truncated and migmatitic raft margins. Rafts of GSP have also been observed in scattered locations throughout the Franklin Mountains (Bradshaw, 1989b, 1990). At Mt Daniel the WFO is in intrusive contact with 129 Ma orthogneiss of the ARC. Bradshaw (1990) described the well-developed igneous features and an intrusive contact with the ARC at this locality.

The WFO shows variable degrees of deformation from relict igneous to granoblastic gneissose textures, and localized late development of hydrous shear foliations. In areas of low strain the WFO preserves relict

igneous clinopyroxene–orthopyroxene assemblages that were variably recrystallized during high-grade metamorphism to clinopyroxene–orthopyroxene–plagioclase-bearing assemblages with or without hornblende, biotite, clinozoisite, K-feldspar and quartz (Bradshaw, 1990; Clarke *et al.*, 2000). In some cases a weak S1 is developed. Similar metamorphic two pyroxene-hornblende assemblages were described from low strain zones within the ARC and were shown to have formed under conditions of $P < 8$ kbar and $T > 750$ °C (Clarke *et al.*, 2000). Clarke *et al.* (2000) concluded that the ARC and WFO were emplaced into the middle to upper crust. It is possible that these S1 two pyroxene-hornblende assemblages reflect auto-metamorphism, associated with deformation during emplacement (e.g. Hollis *et al.*, 2003).

Subsequent development of garnet-bearing replacement textures in both the ARC and WFO record an ensuing high-pressure history as outlined below. In some areas the earliest foliation is cut by garnet-bearing trondjemitic veins. Marginal to these veins garnet reaction zones, typically 1–10 cm wide, are developed in which orthopyroxene is separated from plagioclase, quartz, and K-feldspar by aggregates of fine-grained garnet, clinopyroxene and rutile (Oliver, 1977; Bradshaw, 1989b; Clarke *et al.*, 2000; Daczko *et al.*, 2001b, 2002b). The transition from two pyroxene to garnet-clinopyroxene assemblages has been linked to a pressure increase after WFO emplacement, involving burial from mid (*c.* 25 km) to lower (*c.* 45 km) crustal levels. Mineral thermobarometric constraints require conditions of >750 °C and 12–14 kbar during the development of garnet reaction zones (Bradshaw, 1989b; Clarke *et al.*, 2000). Structural analyses of the deformed garnet reaction zones in northern Fiordland indicate oblique convergence in the lower crustal root of a collisional orogen (Daczko *et al.*, 2001a). Garnet reaction zones in the ARC are deformed by mylonitic shear zones formed under conditions of *c.* 14 kbar and 680 °C (Clarke *et al.*, 2000). Ductile thrusts in the ARC, shear zones in the WFO at Poison Bay, and development of the main gneissose fabric in the ARC at Milford Sound are thought to belong to the same high-pressure upper amphibolite facies structural/metamorphic episode (Clarke *et al.*, 2000; Daczko *et al.*, 2001a). Kyanite–paragonite–phengite-bearing assemblages from the ARC in Milford Sound are consistent with these relatively lower temperature, high-pressure conditions, indicating rapid cooling of these rocks by up to 200 °C after burial and while still at lower-crustal levels (Daczko *et al.*, 2002c).

The WFO is thought to have provided a significant early Cretaceous heat source that resulted in upper amphibolite facies metamorphism and localized melting of the country rocks in northern Fiordland (Bradshaw, 1985, 1989a, 1990; Mattinson *et al.*, 1986; Clarke *et al.*, 2000; Tulloch *et al.*, 2000; Daczko *et al.*, 2001a, 2002a,c; Hollis *et al.*, 2003). However the thermal effects of the WFO are thought to be more localized in central Fiordland. Results of Ar–Ar dating of paragneiss from the Doubtful Sound region show that Ar-loss associated with a Cretaceous thermal event becomes more significant with proximity to Cretaceous plutons. K–Ar cooling ages of 93–77 Ma and the development of Mid-Cretaceous extensional magmatism in Westland are consistent with a rapid change in plate boundary configuration immediately

Table 1. Sample localities and petrography. Mineral abbreviations follow the scheme of Kretz (1983); PG and WFO refers to paragneiss and western Fiordland Orthogneiss, respectively.

Sample	Location	Rock type	Description	Assemblage	Reason sample selected for geochronology
CA90	Crooked arm, Doubtful Sound	WFO	Coarse-grained diorite with no foliation and equilibrated textures	Relict ig: Cpx–opx–pl–ilm–qtz, later hbl–bt	Emplacement age of the WFO
CA10	Crooked arm, Doubtful Sound	WFO	Sheared garnet reaction zone within the WFO	Relict ig: Cpx–opx–pl–rt–qtz $S2^{DS}$: grt–cpx–pl	Development of high-pressure garnet reaction zones in the WFO
9710	George Sound	WFO	Moderately foliated ($S2^{GS}$) coarse-grained dioritic gneiss	$S2^{DS}$: Hbl–bt–ep–pl–qtz–ap–ilm–rt–spn	Emplacement age of the WFO
DAN22	Mt Daniel	WFO	Medium-grained foliated ($S1^{MD}$) flow-banded dioritic gneiss	$S1^{MD}$: Grt–hbl–bt–czo–pl–ilm–qtz	Emplacement age of dioritic intrusive phase of WFO near its margin with the ARC
DAN23	Mt Daniel	WFO	Coarse-grained, weakly foliated trondjhemitic dyke cross-cutting DAN24	Hbl–pl–ep–qtz, late chl–bt	Minimum age of $D1^{MD}$ in WFO
DAN24	Mt Daniel	WFO	Coarse-grained, weakly foliated ($S1^{MD}$) dioritic gneiss	$S1^{MD}$: Hbl–bt–pl–czo–ilm–rt	Emplacement age of massive WFO unit
9713A	George Sound	PG	Medium-grained unfoliated paragneiss from within migmatitic zone	Grt–hbl–bt–czo–qtz–ilm–rt–ttn–ttn	Age of source material for metasedimentary unit and development of $S2^{GS}$ metamorphic assemblage
9705	George Sound	PG	Weakly foliated ($S2^{GS}$) paragneiss	$S2^{DS}$: Grt–hbl–bt–czo–pl–qtz–ttn	Age of source material for metasedimentary unit and development of $S2^{GS}$ metamorphic assemblage
9717B	George Sound	PG	Weakly foliated ($S1^{GS}$) paragneiss	$S1^{GS}$: Grt–st–bt–ms–ky–pl–qtz–rt	Age of source material for metasedimentary unit and development of $S1^{GS}$ metamorphic assemblage
CA39M	Kellard Point, Doubtful Sound	PG	Strongly foliated paragneiss	$S2^{DS}$: Grt–bt–ms–czo–ky–pl–qtz–rt–ttn	Age of source material for metasedimentary unit and development of $S2^{DS}$ metamorphic assemblage

Table 2. Relative timing of deformation features and associated typical metamorphic assemblages at each locality. Magmatic and metamorphic events regarded as synchronous are shaded. Further correlations are not warranted on the basis of structural style alone given the complexity of the terrane and the distances between localities.

George Sound	Doubtful Sound	MT Daniel
$S1^{GS}$ GSP: sub-horizontal foliation in low-strain zones – Grt–bt–st–ms–ky–pl–qtz ± ilm, rt		
WFO	WFO	WFO $S1^{MD}$ WFO: Steep S dipping gneissic foliation with moderate WSW plunging lineation – Hbl–bt–czo–pl–ilm–rt Contact aureole ARC: granoblastic assemblages – Grt–cpx–hbl–czo–pl–qtz
$S2^{GS}$ Pervasive steep NW dipping foliation with moderately plunging lineation, WFO: gneissic foliation – Hbl–plg–bt–ttn–ti–rt–ilm ± cpx, opx GSP: Bt-rich and poor layers – Grt–hbl–bt–pl–qtz ± czo, ilm, rt, ttn		
	GRZ WFO: static recrystallization around Grt-bearing trondjemitic veins – Grt–cpx–opx–plg–qtz–rt	GRZ static recrystallization around g-bearing trondjemitic veins WFO: Grt–cpx–hbl–czo–pl–qtz–ilm–rt ARC: Grt–cpx–hbl–bt–czo–ky–pl–qtz–rt
		$S2^{MD}$ WFO: mylonitic foliation in localized steep SE dipping shear zones, shallow SW plunging lineations – Grt–hbl–bt–pl–qtz
	$S2^{DS}$ Pervasive sub-horizontal shear foliation and shallow NE plunging lineation Paragneiss: Grt–bt–ms–czo–pl–ksp–q–ttn WFO: Cpx–opx–pl–q–ilm, late hbl–bt	

following emplacement of the WFO (Gibson *et al.*, 1988; Tulloch & Kimbrough, 1989).

SAMPLE SETTING AND DESCRIPTION

U–Pb zircon geochronology has been undertaken on samples of the WFO from Mt Daniel, Doubtful Sound, and George Sound and on paragneiss from Doubtful and George Sounds (Fig. 1). At Mt Daniel, where an intrusive contact of the WFO into the ARC is well-exposed, samples were selected to determine the age of emplacement and deformation in the WFO. At George Sound an intrusive contact is also exposed between the WFO and the GSP sequence, which is migmatized in the contact zone. At this locality both WFO and samples of the GSP were collected to determine the age of emplacement of the WFO, the detrital zircon signature of the paragneiss and the age of metamorphism of the GSP. In Doubtful Sound the WFO is juxtaposed against a paragneiss sequence along the Doubtful Sound shear zone. Samples of the WFO were collected to determine the age of emplacement and the development of high-pressure garnet reaction zones and a sample of paragneiss within the shear zone was collected to determine the detrital zircon signature of the paragneiss and the age of development of the metamorphism associated with shearing.

A short description of each locality is given below. The petrography of individual samples and the reason each sample was selected for geochronology are listed in Table 1. A summary of the deformation features, associated metamorphic assemblages, and correlations of these between localities is given in Table 2.

Mt Daniel (DAN24, DAN23, DAN22 and MD12)

At Mt Daniel there is continuous exposure across an intrusive contact of the early Cretaceous WFO with the ARC. Here primary magmatic structures are well preserved and overprinted by granulite facies metamorphic assemblages. The section is divided into four broad structural and lithological domains. From outside the WFO batholith to within (north to south), these include: (i) the 136–129 Ma ARC (Hollis *et al.*, 2003), structurally below the WFO, (ii) a contact aureole, (iii) a margin zone of sheeted intrusions and dykes, and (iv) a moderately deformed massive WFO unit. The ARC immediately north of Mt Daniel is weakly foliated dioritic gneiss, largely comprised of hornblende, clinozoisite, biotite and plagioclase with minor garnet, quartz and rutile. Within the contact aureole (*c.* 200–250 m wide), ARC gneiss are intruded by tonalitic to gabbroic igneous phases of WFO (e.g. see Fig. 8 in reference Bradshaw, 1990). In the base of the contact aureole rafts of weakly foliated ARC, in some cases migmatitic, occur within the WFO. Approaching the main body of the WFO is a zone of synkinematic tonalitic and trondjemitic sheets. Subordinate mafic dykes, metamorphosed to amphibolites and commonly folded, cut the granitic sheets towards the top of the sheeted section. Structurally above these is a coarse-grained hornblende cumulate that grades upward into a zone of dioritic (sample DAN22) and gabbroic intrusions that are also cut by trondjemitic dykes (sample DAN23). These dykes are relatively common throughout the WFO and also the ARC (e.g. Clarke *et al.*, 2000; Daczko *et al.*, 2002b) and occur as centimetre to metre-width dykes that are laterally continuous on a metre to hundred metre scale. Typically they comprise medium to coarse-grained plagioclase and quartz with minor epidote and hornblende. These cut a well-developed foliation ($S1^{MD}$) in the host WFO. This may be a reworked magmatic foliation. $S1^{MD}$ is commonly defined by aligned and elongate clusters of mafic minerals in a dominantly plagioclase feldspar matrix. Mafic mineral clusters most commonly comprise

coarse calcic-amphibole, clinozoisite and minor ilmenite with or without biotite and rutile.

The zone of dioritic and gabbroic intrusions finally give way to the massive WFO unit (sample DAN24), which also holds a well-developed steeply S dipping $S1^{MD}$ with a moderately WSW plunging mineral lineation. Localized $D2^{MD}$ shear zones cut $S1^{MD}$ and post-$D1^{MD}$ trondjemitic dykes, and show assemblages similar to those of $S1^{MD}$ though some are also garnet-bearing. D2 shear zones are steeply SE dipping with shallow SW plunging mineral and stretching lineations. The WFO is cut by late epidote-lined fractures and pegmatite dykes.

Doubtful Sound (CA10, CA90 and CA39M)

In Doubtful Sound the sub-horizontal, 1–2 km thick Doubtful Sound shear zone juxtaposes the WFO (samples CA90 & CA10) and the tectonically overlying ortho- and paragneiss (sample CA39M). Lithologies of both rock units show well-developed $S2^{DS}$ fabrics associated with the shear zone and become more hydrous and finer-grained with proximity to the shear zone. Within the shear zone various orientations of garnet-bearing trondjhemitic veins (some with associated reaction zones) show mutually cross-cutting relationships and are variably deformed by the shear zone fabric (sample CA10; Oliver, 1980; Harnmeijer, 2001). Distal to the shear zone these occur in sub-vertical orientations, but have undergone flattening and rotation within the shear zone to sub-horizontal orientations ($S2^{DS}$; Harnmeijer, 2001). $S2^{DS}$ assemblages in the paragneiss typically comprise quartz, plagioclase, biotite and K-feldspar, muscovite, garnet, clinozoisite, and titanite. Marbles intercalated with calc-silicate gneiss are comprised of calcite, diopside, scapolite, K-feldspar, garnet and muscovite. Orthogneiss vary from quartzofeldspathic, to biotite-rich to hornblende-rich $S2^{DS}$ assemblages with intercalated calc-silicate gneiss, amphibolite and quartzite (Oliver, 1980; Harnmeijer, 2001).

George Sound (9710, 9713A, 9705 and 9717B)

The GSP comprises a sequence of pelitic, psammitic and subordinate calc-silicate gneiss. An extensive continuous section of the GSP crops out over a 3 km length of coastline near the mouth of George Sound (Fig. 1; Bradshaw, 1990). The main body of the GSP is separated from the WFO by a 300 m wide zone of migmatitic gneiss that forms a compositional gradient between the paragneiss and the WFO. Samples of the GSP were taken both within the migmatite zone (sample 9713A) and in the main body of the GSP (sample 9705). A pervasive steeply NW dipping foliation ($S2^{GS}$) and moderately plunging lineation ($L2^{GS}$) affects the GSP and WFO alike, though an earlier sub-horizontal foliation ($S1^{GS}$) is preserved only in low-strain zones within the GSP (sample 9717B). In the WFO $S2^{GS}$ is defined by recrystallized, aligned hornblende in largely hornblende-plagioclase dioritic gneiss with accessory biotite, titanite, rutile, ilmenite (sample 9710) and rare clinopyroxene and orthopyroxene. The WFO is generally massive in texture, though in places intersheeting of mafic and felsic layers is thought to represent relict igneous flow-banding (Bradshaw, 1990; Degeling, 1997). In the GSP $S2^{GS}$ is expressed as compositional layering defined by biotite-rich and poor layers with assemblages including garnet, hornblende, plagioclase, quartz, clinozoisite, muscovite, biotite, kyanite, staurolite and rutile.

ANALYTICAL TECHNIQUES

Samples were crushed and separated into density fractions using heavy liquids at the CSIRO Materials Division at North Ryde, Sydney. Zircon was hand-picked from the heaviest fraction with the aid of an ultra-violet (UV) light microscope, and mounted in epoxy, along with sensitive high-resolution ion microprobe (SHRIMP) zircon standard material, and polished until exposed through their mid-sections. Cathodoluminescence (CL) and back-scattered electron (BSE) imaging were carried out on all samples to characterize internal structures arising from growth and/or metamorphism and to identify any inclusions or defects for the purpose of choosing appropriate sites for analysis. CL imaging was carried out on a Hitachi S-2250N SEM at the Australian National University (ANU) Electron Microscopy Unit and a JEOL 35C SEM with attached Oxford Instruments MonoCL imaging and spectral analysis system at the University of Technology, Sydney. BSE imaging was carried out on a Cambridge S360 SEM at the ANU Electron Microscopy Unit and a Philips SEM505 at the Key Centre for Electron Microscopy at the University of Sydney. Some of the rims on zircon cores identified using CL imaging were too small ($< 20\ \mu m$) for analysis using the conventional method. These were remounted in epoxy and lightly polished so that the rims were just exposed on the surface of the mount. Analyses were carried out by depth profiling through the rims rather than through grains polished through their mid-section, giving a broader area of rim material for analysis.

U-Th-Pb isotopes were analyzed on SHRIMP I and SHRIMP RG (Reverse Geometry) at the ANU with standard operating techniques (Muir *et al.*, 1996). A 3–5 nA mass-filtered O_2^- primary beam was focussed into a 30 μm diameter spot to sputter material from the sample to form a 30 μm diameter flat-bottomed crater. Prior to analysis the primary beam was rastered over the sample area for two minutes to clean the surface. Positive ions were extracted and mass separated via cyclical stepping of the magnet into the peaks of interest: $^{90}Zr_2^{16}O$, ^{204}Pb, ^{206}Pb, ^{207}Pb, ^{208}Pb, ^{238}U, $^{232}Th^{16}O$ and $^{238}U^{16}O$. Pb isotopic ratios were taken as measured; no corrections have been applied for isotopic mass fractionation or Pb hydride interferences, because any corrections would have a negligible effect on this data set. U–Pb ratios were normalized to UO/U and calibrated to 417 Ma zircon from the Temora granite, NSW. Uncertainties are largely dominated by the counting statistics of the individual measurement of the Temora standard. The final error in the mean of the standards was propagated on to the final sample age determination.

The uncorrected data for all orthogneiss samples are presented as Tera–Wasserberg concordia diagrams, on which measured ratios are plotted with respect to the $^{207}Pb/^{206}Pb$–$^{238}U/^{206}Pb$ concordia. $^{238}U/^{206}Pb$ ages are considered reliable in cases in which data fall close to concordia and there is no evidence for significant Pb-loss. In the case of Phanerozoic zircon $^{238}U/^{206}Pb$ ages are regarded as more reliable than $^{235}U/^{207}Pb$ or $^{207}Pb/^{206}Pb$ ages because of the low proportion of available ^{235}U, resulting in only small proportions of radiogenic ^{207}Pb. Given the low count rates from ^{204}Pb and ^{207}Pb, using a $^{204}Pb/^{206}Pb$ common lead correction would result in significant error propagation into $^{207}Pb/^{206}Pb$ age calculations. Thus in this study the $^{207}Pb/^{206}Pb$ ratio was used to monitor common Pb ($^{207}Pb/^{206}Pb$ correction method of Muir *et al.*, 1996) and each datum was assumed to be a simple mixture of common and radiogenic Pb. $^{238}U/^{206}Pb$ ages were calculated by extrapolating from the common Pb isotopic value, determined from the Cumming & Richards (1975) model Pb growth curves, through the measured datum onto concordia. Age data for each sample are quoted with a two SD uncertainty and individual ages for each analysis are quoted with a one SD uncertainty. Probability diagrams are presented for samples that show significant spread in the age populations as a result of detrital zircon or inheritance. These curves represent the summation of unit–area Gaussian curves for all data from a sample.

SHRIMP U–Pb ZIRCON RESULTS

U and Th concentrations, isotopic ratios and age data for each analysis are summarized in Table S1 which is available at http://www.blackwellpublishing.com/products/journals/suppmat/jmg/jmg537/jmg537sm.htm. Representative images of the characteristic zircon morphologies observed in CL are shown in Fig. 2. Graphical representations of the uncorrected data are presented in Fig. 3.

Western Fiordland Orthogneiss

Mt Daniel (DAN24, DAN23 and DAN22)

Zircon from homogeneous dioritic WFO sample *DAN24* is colourless to pale pink and fluoresce strongly yellow in UV light. Grains are generally 150–250 μm in length, with aspect ratios of 1:1, and are anhedral and very angular. They have a strong CL response, which generally shows patchy bright and darker areas (fir-tree sector zonation) with no strong indication of any core-rim structure Fig. 2a). However, some grains show remnant oscillatory zonation, and where present this illustrates that the grains are usually highly fragmented. The data are slightly overdispersed to younger ages (consistent with partial Pb loss) and 20 of 22 grains give a $^{238}U/^{206}Pb$ age of 121.8 ± 1.7 Ma (2σ, MSWD = 1.32; Fig. 3a). Uranium concentrations range from 110 to 960 ppm, Th concentrations from 75 to 400 ppm, and Th/U range from 0.42 to 1.18.

Sample *DAN23*, a post-D1 trondjemitic dyke in the WFO, contains colourless to pale pink zircon that show generally weak yellow fluorescence in UV light, though a few grains show strong fluorescence. The zircon is euhedral and commonly broken into two or more fragments. Grains range in length from 150 to 250 μm with aspect ratios of 1:1 to 1:4, but generally *c*. 1:3. CL imaging reveals partially preserved weak oscillatory zonation in most zircon, often overprinted by weak sector zonation. In some cases the grains appear almost homogeneous. The analyses are overdispersed for a single population. One grain gives a considerably older age of *c*. 340 Ma (with anomalously high U at 270 ppm and low Th/U at 0.54), and a further grain is resolved at *c*. 150 Ma (160 ppm U and Th/U of 0.22). It is not possible to distinguish whether the younger age represents mixing (Pb loss) with the older component or whether it represents a distinct event. Either situation is geologically reasonable. Of the remaining analyses, one low precision analysis is resolved from the younger side of the population. Seventeen of 20 analyses give a $^{238}U/^{206}Pb$ age of 123.6 ± 3.0 Ma (2σ, MSWD = 0.58; Fig. 3b). U concentrations of the magmatic population range from 36 to 110 ppm, Th from 33 to 150 ppm and Th/U range from 0.79 to 1.42.

The presence of some Palaeozoic material in the protolith to the WFO at Mt Daniel is further indicated from sample *DAN22*, a flow-banded dioritic WFO sample. Zircon from *DAN22* is pink and fluoresce weakly yellow in UV light. Grains are elongate, euhedral to subhedral with rounded terminations. They are 100–200 μm in length with aspect ratios of 1:2 to 1:3. CL imaging reveals oscillatory zoned cores with thin bright rims generally < 5 μm but up to 20 μm (Fig. 2c). Fourteen analyses of oscillatory zoned cores give $^{238}U/^{206}Pb$ ages in the range 366–239 Ma (Fig. 3c) with U concentrations ranging from 110 to 340 ppm, Th from 47 to 250 ppm, and Th/ U ratios from 0.31 to 0.84. Two analyses of the bright rims give younger $^{238}U/^{206}Pb$ ages of 126.5 ± 5.9 and 122.2 ± 4.1 Ma (Fig. 3c) with U concentrations of 67 and 160 ppm, Th of 23 and 28 ppm and Th/U ratios of 0.34 and 0.17, respectively. DAN22 most likely represents an orthogneiss dominated by Palaeozoic protolith with metamorphic overgrowths apparent at *c*. 126 Ma.

Doubtful Sound (CA90 and CA10)

Zircon from *CA90*, a dioritic WFO, is colourless and fluoresce strongly yellow in UV light. They are subhedral to anhedral and are often fragmented. Grains range from 100 to 200 μm in length with aspect ratios of 1:1 to 1:2. Zircon has a dull generally homogeneous CL response with no indication of a core-rim structure (Fig. 2d). In a very few cases there is evidence for weakly preserved oscillatory zonation. All twelve analyses give a $^{238}U/^{206}Pb$ age of 115.6 ± 2.4 Ma (2σ, MSWD = 0.79; Fig. 3d). U concentrations range from 74 to 190 ppm, Th from 52 to 210 ppm, and Th/U range from 0.70 to 1.21.

CA10 is a sample of a sheared garnet reaction zone within the WFO. Zircon from CA10 is in relatively low abundance. They are colourless to pale pink and fluoresce strongly yellow in UV light. Grains are subhedral and slightly rounded, with aspect ratios of 1:1 to 1:1.5. They range in length from 40 to 100 μm. As in sample CA90, zircons typically have a dull, homogeneous CL response, with no indication of a core-rim structure (Fig. 2e). In a few cases there is evidence for weakly preserved oscillatory zonation. All twelve analyses are included to give a $^{238}U/^{206}Pb$ age of 114.0 ± 2.2 Ma (2σ, MSWD = 1.25; Fig. 3e). Eleven analyses show U concentrations in a range from 100 to 450 ppm, Th from 73 to 430 ppm, and Th/U ratios range from 0.47 to 1.19. One analysis has low Th with U at 180 ppm and Th/U at 0.0007 suggestive of a metamorphic origin, but its age is not detectably younger.

George Sound (9710)

Zircon from sample 9710, a dioritic WFO, is pink and fluoresce strongly yellow in UV light. Grains are anhedral to subhedral, angular and fragmented. They have aspect ratios of 1:1 to 1:2.5 (typically 1:1) and range in length from 150 to 300 μm. The grains have a generally dull homogeneous CL response with no indication of any core-rim structure (Fig. 2f). All 16 analyses are included to give a $^{238}U/^{206}Pb$ age of 120.0 ± 2.6 Ma (2σ, MSWD = 0.62; Fig. 3f). Uranium concentrations range from 85 to 340 ppm, Th from 55 to 390 ppm, and Th/U range from 0.65 to 1.15.

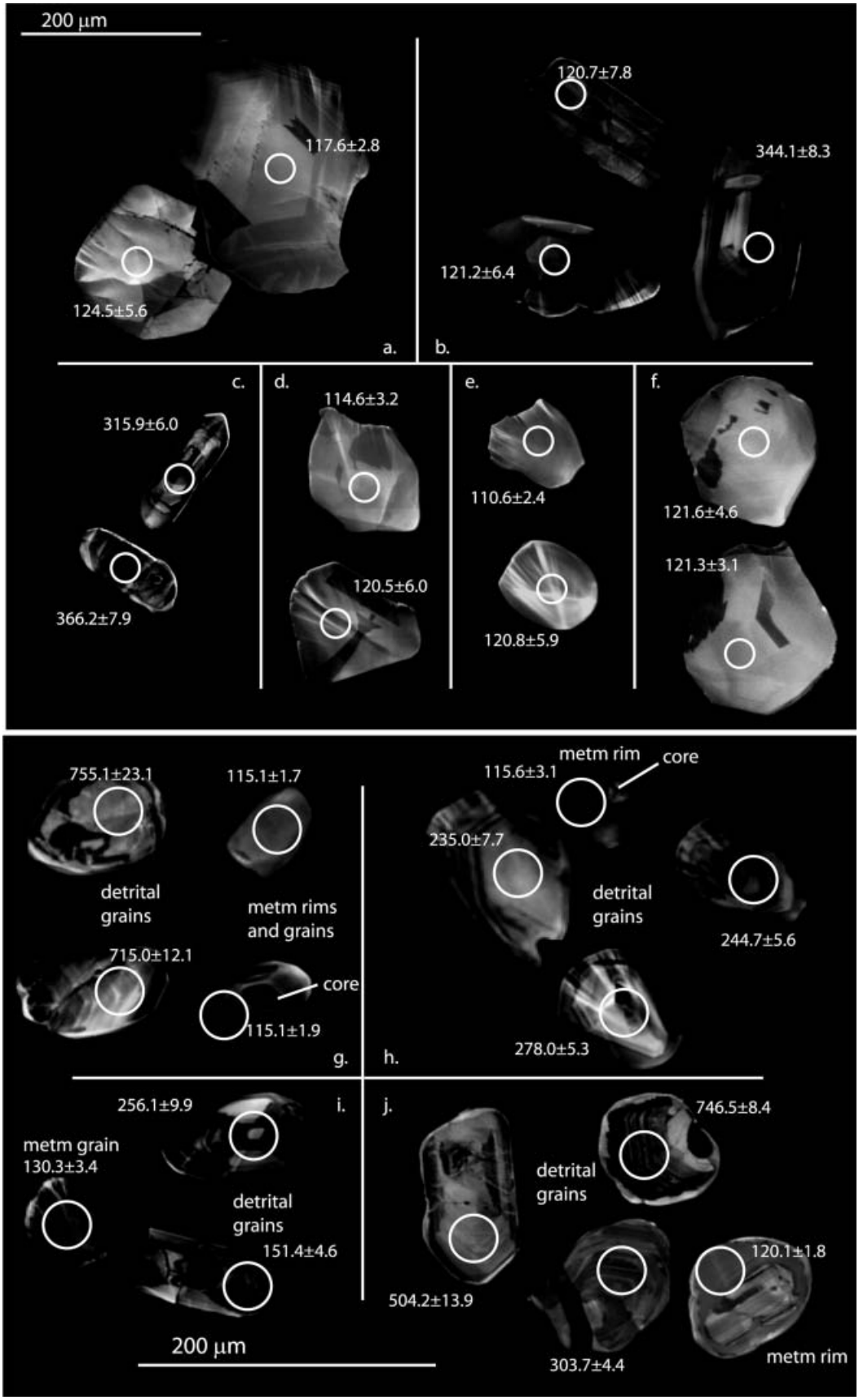

Paragneiss

Doubtful Sound (CA39M)

Sample *CA39M*, a strongly foliated paragneiss, contains colourless zircon that fluoresces strongly yellow in UV light. They are subhedral to rounded with aspect ratios of 1:1 to 1:2 and generally 1:2. Grains range in length from 30 to 100 μm. CL imaging shows that the majority of grains preserve oscillatory zonation (in some cases slightly irregular) typically truncated by homogeneous relatively bright rims that range from 5 to 40 μm in width. A few small grains give a dull homogeneous CL response with no evidence of any core-rim structure (Fig. 2g). Fifty-one analyses give a total age range from almost 3000 to 110 Ma. Forty-one of the analyzed grains consist of oscillatory-zoned cores that give $^{238}U/^{206}Pb$ ages ranging from nearly 3000 to 180 Ma. In the probability density function there are distinct peaks at *c*. 600–500 Ma and 1100–900 Ma (Fig. 3h): the pattern is similar to the lower Palaeozoic zircon-age signature from the Gondwana margin including the Greenland Group (Ireland & Gibson, 1998). Uranium concentrations for these grains range from 14 to 1300 ppm, Th from 21 to 780 ppm, and Th/U from 0.09 to 1.68. Ten analyses of homogeneous rims and small grains give Cretaceous ages in the range 126–106 Ma with Th/U ranging from 0.02 to 1.40. A single analysis at 138 Ma is removed from the main age group. The remaining nine analyses yield a weighted mean of 117.7 ± 2.8 Ma (2σ, MSWD = 2.60; Fig. 3g) with U concentrations ranging from 225 to 1299 ppm, Th from 11 to 558 ppm, and Th/U from 0.02 to 1.40, generally <0.2. The weighted mean shows excess dispersion (MSWD = 2.60) suggesting that more than one population may be present, though this is difficult to resolve with the available data. The probability density function indicates two peaks at *c*. 120 and *c*. 115 Ma. The five youngest analyses give a weighted mean age of 114.9 ± 2.2 Ma (2σ, MSWD = 0.77) and have U concentrations from 382 to 1120 ppm, Th from 11 to 183 ppm, and Th/U from 0.02 to 0.16 (three of which have Th/U <0.05). The four older analyses have a weighted mean age of 120.8 ± 2.3 Ma (2σ, MSWD = 0.94) and U concentrations of 225–1299 ppm, Th of 37–558 ppm, and Th/U ranging from 0.11 to 1.40. The combined chemistry and age characteristics therefore are consistent with two metamorphic age components. This inference is also consistent with the depth profiles through the rims of three grains that give ages of 115.7 ± 7.2 (2σ, U =273 ppm, Th/U = 0.12), 117.9 ± 5.0 Ma (2σ, U = 633, Th/U = 0.03), and 127.2 ± 8.4 Ma (2σ,U = 711 ppm, Th/U = 0.05).

George Sound paragneiss (9713A, 9705 and 9717B)

9713A is an unfoliated migmatitic gneiss from within the contact zone between the WFO and GSP. 9713A contains pink zircon that fluoresces strongly yellow in UV light. Grains are generally either rounded and equant or elongate with euhedral but slightly rounded terminations and aspect ratios of *c*. 1:2.5. Zircons range from 100 to 150 μm in length. CL imaging shows oscillatory-zoned cores that are often truncated by thin relatively bright homogeneous rims, 5–30 μm in diameter (Fig. 2h). A few small grains give a dull homogeneous CL response with no evidence for a core-rim structure. Eighty-seven analyses show a total age range from 115 to 450 Ma. The probability density plot is bimodal with a broad spread of ages peaking in the span of 200–300 Ma, and a well-defined younger peak at *c*. 120 Ma (Fig. 3j). The younger peak is defined by 15 analyses in the age range of 127 to 103 Ma. Of these, 103 Ma is represented by a single analysis and two analyses at 127 Ma are also resolved from the main peak. The remaining 12 analyses yield a weighted mean of 117.2 ± 1.3 Ma (2σ, MSWD = 1.77; Fig. 3i) with U concentrations ranging from 220 to 590 ppm, Th from 12 to 160 ppm, and Th/U from 0.23 to 0.36 with one low value at 0.02. Depth profiles through four grains give a spread of ages from 98 to 121 Ma with three analyses clustering around the mean of the Cretaceous peak.

The remaining (older) analyses of 9713A show a wide spread of ages inconsistent with a small number of components. Most of the analyses are of oscillatory-zoned cores that give $^{238}U/^{206}Pb$ ages ranging from late Ordovician to late Jurassic in age with the majority of grains Permian to Triassic in age. U concentrations range from 130 to 1300 ppm, Th from 44 to 1700 ppm, and Th/U from 0.13 to 1.47. The majority of analyses have 200–500 ppm U, 20–400 ppm Th, and Th/U between 0.3 and 0.9. The issue for this sample is whether the range in ages represents the distribution from a wide range of sources (i.e. a paragneiss), or whether the range in ages is produced from variable Pb loss from an igneous protolith (i.e. an orthogneiss). Given the zircon age data in isolation the paragenesis of this sample (i.e. sedimentary *v*. magmatic origin) is difficult to establish. The presence of an Ordovician age is indicative of a sedimentary input (though it represents a very small fraction of the material analyzed) and apparent dips in the age probability curve at *c*. 270 and 220 Ma define peaks in the spectrum similar to sedimentary age curves. However the form of the distribution curve is similar to that of DAN22 which, on the basis of field relationships and composition, is interpreted as an orthogneiss. Again in this case, other

Fig. 2. Cathodoluminescence (CL) images of representative zircon morphologies from: (a) massive dioritic WFO, Mt Daniel – DAN24, (b) post-D1MD trondjemitic dyke – DAN23, (c) dioritic WFO intrusive phase near margin with ARC – DAN22, (d) dioritic WFO, Doubtful Sound – CA90, (e) garnet reaction zone in WFO, Doubtful Sound – CA10, (f) dioritic WFO, George Sound – 9710, (g) paragneiss, Doubtful Sound – CA39M, (h) migmatitic paragneiss, George Sound – 9713A, (i) paragneiss from main body of GSP, George Sound – 9705, and (j) paragneiss from low strain zone, George Sound – 9717B.

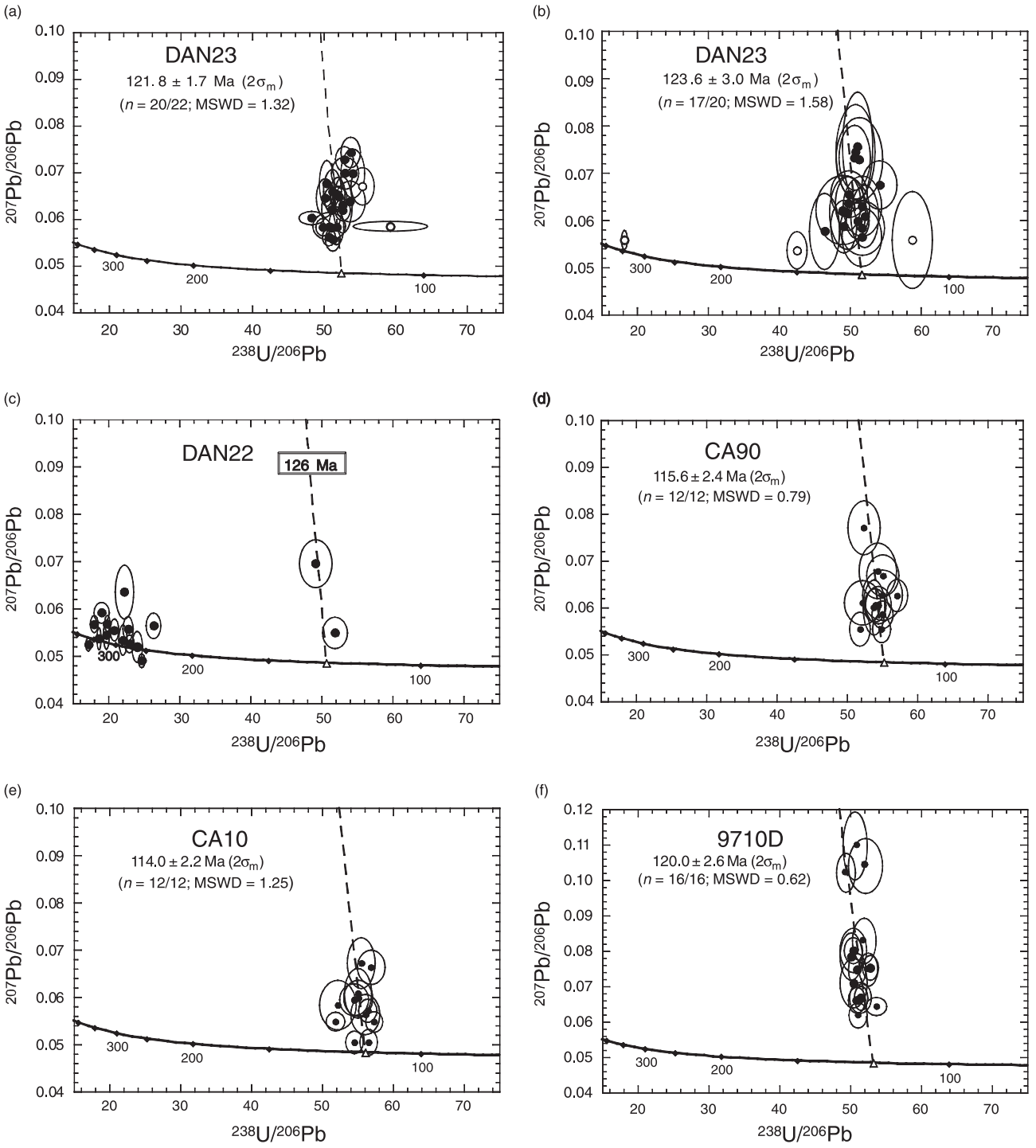

Fig. 3. Tera-Wassaberg plots (TW) and cumulative relative probability diagrams (CP) of SHRIMP zircon data for (a) DAN24 – TW, (b) DAN23 – TW, (c) DAN22 – TW, (d) CA90 – TW, (e) CA10 – TW, (f) 9710 – TW, (g) CA39M – TW, (h) CA39M – CP, (i) 9713A – TW, (j) 9713A – CP, (k) 9705 – TW, (l) 9705 – CP, (m) 9717B – TW, and (n) 9717B – CP. The inset in (n) shows an enlargement of the Phanerozoic age spectrum for 9717B.

factors are important in establishing the derivation of the zircon population from this sample: the field occurrence (layered paragneiss sequence intruded by WFO) and mineralogy (garnet, hornblende, biotite, clinozoisite, quartz, ilmenite, rutile, titanite; Table 1) are consistent with a sedimentary origin. Given the extensive production of metamorphic rims in this rock, it is likely that at least some disturbance in U–Pb systematics is inevitable, possibly accounting for the observed spread in the distribution curve.

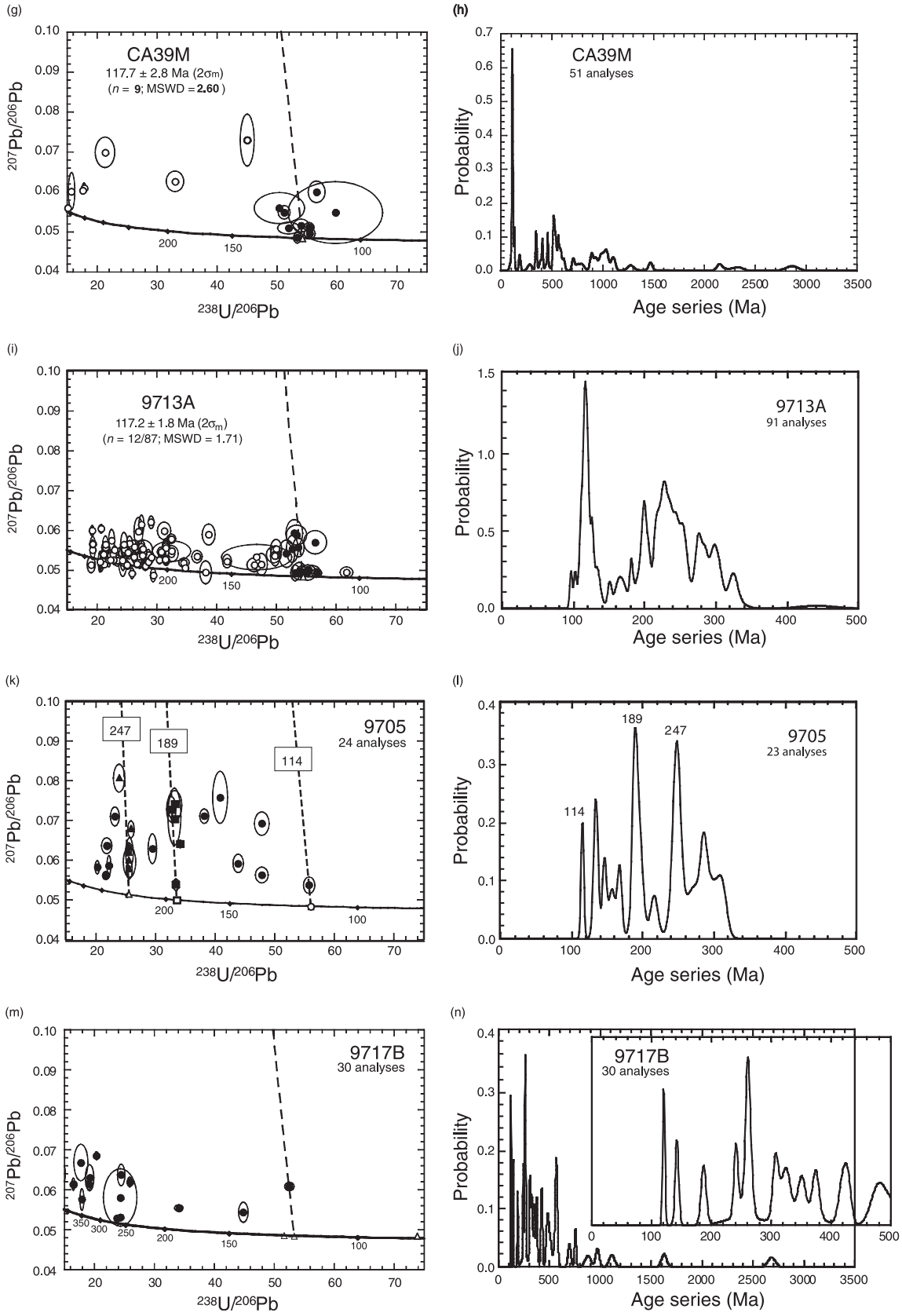

Fig. 3. *Cont'd.*

9705 is a weakly foliated gneiss from within the main body of the GSP, and has zircon that is pink and fluoresces yellow in UV light. Grains are rounded, generally with aspect ratios of 1:1 but up to 1:2, and range from 40 to 150 μm in length. CL imaging shows oscillatory-zoned cores with thin homogeneous rims of 10–50 μm (Fig. 2i). A few small grains give a dull homogeneous CL response with no evidence for a core-rim structure. Twenty-one analyses of oscillatory-zoned cores give late Carboniferous to early Cretaceous $^{238}U/^{206}Pb$ ages, though most fall in the Permian to Triassic, similar to the age spectra of sample 9713A (Fig. 3l). Uranium concentrations range from 74 to 1700 ppm, Th from 16 to 370 ppm, and Th/U ratios from 0.12 to 1.11. Two analyses of small homogeneous grains give younger Cretaceous ages of 132.2 ± 3.0 and 130.3 ± 3.4 Ma (Fig. 3k) with Th/U ratios of 420:0.01 and 86:0.42, respectively. The systematics of 9705 are therefore rather similar to 9713A. However, in 9705 two age peaks at *c.* 250 and *c.* 190 Ma are apparent comprising five and six analyses, respectively. The coincidence of a significant number of analyses such as this would normally be taken as indicative of distinct age components. This possibility can not be ruled out and on the basis of the zircon age spectra sample 9705 appears the most likely to have a significant sedimentary component. However, given the likely effects of Pb redistribution on these zircons, it is also possible that these peaks are coincidental.

9717B is a weakly foliated ($S1^{GS}$) paragneiss from a low-strain zone wrapped by $S2^{GS}$ in the GSP. Zircon is pink and fluoresces yellow in UV light. Grains are rounded, typically with aspect ratios of 1:1 to 1:2, and range from 80 to 180 μm in length. CL imaging shows oscillatory-zoned cores with very thin homogeneous rims of <10 μm (Fig. 2j). Twenty-nine analyses of oscillatory-zoned grains give $^{238}U/^{206}Pb$ ages ranging from the Archean (2156.6 ± 101.8 Ma) to early Cretaceous (141.4 ± 2.5 Ma) and with significant peaks at *c.* 550 Ma, *c.* 250 Ma, and *c.* 1000–800 Ma (Table S1; Fig. 3n). Th/U are in the range 0.07–1.94. One analysis of a thin rim gives a metamorphic age of 120.1 ± 1.8 Ma with a Th/U of 0.06 (Fig. 3m). It is likely that there are several age components in this rock. The ages including and older than *c.* 500 Ma are consistent with the local sedimentary input of Gondwana margin greywacke. The youngest ages on rims indicate metamorphism associated with the emplacement of the WFO. The remaining scattered ages are insufficient in number to determine whether components from Carboniferous to Devonian granites are present and whether there is a Permo-Triassic sedimentary component.

Synopsis

Zircon from three samples of dioritic WFO from Mt Daniel, George and Doubtful Sounds show close similarities in morphologies, chemistry and age data. Zircon from DAN24, CA90 and 9710 are anhedral to subhedral and angular with typical aspect ratios of 1:1. They generally have dull homogeneous CL responses, sometimes exhibiting fir-tree sector zonation and rare weak oscillatory zonation. Where present the latter shows that grains are often fragmented. The ages of the three samples, interpreted as emplacement ages, are 121.8 ± 1.7 (DAN24), 115.6 ± 2.4 (CA90), and 120.0 ± 2.6 Ma (9710).

Samples of a flow-banded diorite (DAN22), and a post-D1 trondjemitic dyke (DAN23) from within the WFO at Mt Daniel illustrate considerable complexity in zircon age systematics at this locality, a departure from the norm for WFO age data. The post-D1 dyke (DAN23) gives an emplacement age of 123.6 ± 3.0 Ma, within error of the massive dioritic host gneiss (DAN24). One much older grain from the dyke, 344.1 ± 8.3 Ma, indicates a minor component of inheritance. The flow-banded diorite (DAN22) has a zircon population dominated by an inherited component: oscillatory-zoned grains range in age from 366 to 239 Ma, some with thin bright rims of Cretaceous age (126.5 ± 5.9 and 122.2 ± 4.1 Ma). The dominance of inherited zircon is unusual for a diorite and, considered in isolation, suggestive of a sedimentary origin. However given its field occurrence as a sheeted magmatic body within the WFO (see Sample setting and description section) and its dioritic composition it is interpreted here as a magmatic body largely derived from a Palaeozoic protolith and metamorphosed during Cretaceous emplacement of the WFO.

Zircon from a sheared garnet reaction zone within the WFO at Doubtful Sound (CA10) shows identical morphological and chemical characteristics to those of the main body of the WFO at this locality (CA90). The age of sample CA10, 114.0 ± 2.2 Ma, falls within error of that of CA90. These results are consistent with either (i) no new zircon recrystallization or new growth during garnet reaction zone formation and/or (ii) formation of garnet reaction zones immediately after WFO emplacement. On the basis of the absence of any recrystallization or regrowth features and the consistency of zircon morphology, chemistry and age data between samples CA90 and CA10 the former interpretation is preferred.

The paragneiss sample from Doubtful Sound (CA39M) has a detrital zircon age spectra in the range 2892–349 Ma with prominent peaks at 1100–900 Ma and 600–500 Ma. Thin bright rims and depth profiles through grain rims give Cretaceous ages (dominantly 120–115 Ma), consistent with the age of WFO emplacement at this locality (115.6 ± 2.4, CA90). Paragneiss from George Sound show similarities to some WFO orthogneiss (Cretaceous rims and a Palaeozoic inheritance pattern), but have peaks in their abundance patterns in the Permo-Triassic that could be indicative of a sedimentary input, consistent with their field occurrence and mineralogy. A third sample (9717B) shows a largely Proterozoic detrital age

spectra, similar to the Doubtful Sound paragneiss, with significant peaks at *c.* 1000–800, 560 Ma and two older grains: 1373.1 ± 13.5 and 2156.6 ± 101.8 Ma. This sample also contains several Permo-Triassic aged zircon. One analysis of a homogeneous rim gives a metamorphic age of 120.1 ± 1.8 Ma. The question of whether a Permo-Triassic sedimentary component is indeed present in these rocks is discussed further below.

There is a general trend toward lower Th/U (*c.* <0.2) in zircon interpreted to be of metamorphic origin in both orthogneiss (DAN22) and paragneiss samples (CA39M, 9713A, 9705, 9717B) compared with Th/U in zircon interpreted, on the basis of morphology and host lithology, as magmatic, inherited or detrital. This is typical of zircon geochemistry of metamorphic compared with magmatic zircon in general (e.g. Rubatto & Gebauer, 2000). However, significant variation in Th/U in metamorphic zircon, from 0.02 to 1.40, is also apparent (e.g. samples 9705, 9713A, CA39M, and DAN22). High Th/U zircon interpreted as metamorphic have previously been reported in other terranes (Williams & Claesson, 1987) and bulk rock composition (and probably many other factors) plays an important role.

MINERAL CHEMISTRY AND THERMOBAROMETRY

In previous studies, we have carefully documented the *P–T* history of the early Cretaceous ARC in northern Fiordland (Clarke *et al.*, 2000; Daczko *et al.*, 2001a, 2002c) and to a lesser extent the western Fiordland Orthogneiss at Caswell Sound (Daczko *et al.*, 2002a). These studies presented a common *P–T* history for Fiordland that involved:

(1) Emplacement of the igneous protoliths of the ARC (136–129 Ma) and WFO (126–114 Ma) at $P < 8$ kbar coeval with upper amphibolite facies metamorphism to contact zone partial melting of country rocks and two pyroxene–hornblende granulite facies auto-metamorphism of the plutons;

(2) Collisional-style orogenesis, burial (by >20 km) and high-pressure (12–14 kbar) granulite facies metamorphism, including some partial melting and development of garnet reaction zones;

(3) High-pressure cooling of the eastern margin of the terrane by up to 200 °C during the waning stages of collision;

(4) Decompression, uplift and termination of metamorphism ($T <$ 300–400 °C) by 90 Ma.

Below is outlined the mineral chemistry of some important lithologies from Doubtful and George Sounds (see Table 1 for assemblage information for specific samples). The *P–T* estimates are presented for samples from these units (Table 4) and, along with thermobarometry results reported in Daczko *et al.* (2002b)) for Mt Daniel, these are keyed to the four-stage history determined in previous work and outlined above.

Mineral chemical compositions were determined using a Cameca SX50 Microprobe at the University of New South Wales running with an accelerating voltage of 15 kV, a beam current of 20 nA, and a beam width of 1–3 μm. Elemental concentrations were calculated using the Cameca PAP correction program. Representative analyses of important minerals from the main lithologies are given in Table 3. Mole proportions of pyroxene end members were

Table 3. Representative microprobe analyses of minerals from some important rock types.

	DS08C:WFO					DS40C:S2^{DS} PG				9717B:S1^{GS} PG				9705C:S2^{GS} PG						
	grt	cpx	hbl	bt	pl	grt	hbl	bi	cz	pl	g	st	bt	mu	pl	grt	hbl	bt	ep	pl
SiO_2	39.06	51.78	40.46	36.85	63.24	37.82	39.33	35.22	37.42	60.99	38.13	27.55	37.65	46.64	61.69	37.48	42.62	36.39	37.74	59.25
TiO_2	0.05	0.23	0.83	4.66	0.00	0.03	0.86	2.18	0.10	0.00	0.01	0.60	1.66	0.87	0.00	0.04	0.81	2.46	0.14	0.06
Al_2O_3	21.72	4.72	14.89	15.12	23.48	21.16	14.42	16.61	25.20	24.53	21.70	53.30	18.36	35.39	24.22	21.39	15.72	17.12	21.33	25.34
Cr_2O_3	0.01	0.03	0.03	0.00	0.03	0.04	0.00	0.00	0.04	0.01	0.07	0.03	0.02	0.01	0.00	0.00	0.05	0.01	0.02	0.05
FeO	24.02	6.76	14.48	14.03	0.01	25.48	15.69	16.01	10.02	0.08	31.27	11.37	13.42	1.04	0.02	27.14	12.72	15.43	24.13	0.00
MnO	0.48	0.00	0.12	0.03	0.00	4.65	0.41	0.27	0.36	0.01	0.45	0.04	0.03	0.00	0.03	0.96	0.08	0.09	1.50	0.00
MgO	7.53	12.14	10.55	14.07	0.00	4.80	10.02	12.18	0.00	0.00	6.42	2.19	15.17	1.42	0.00	3.89	10.48	12.22	3.03	0.00
CaO	7.74	21.27	11.67	0.04	4.32	6.14	11.25	0.08	23.43	6.14	2.54	0.01	0.03	0.00	5.34	8.09	11.39	0.06	11.53	6.80
Na_2O	0.03	1.75	1.68	0.15	8.83	0.02	1.80	0.13	0.01	8.29	0.03	0.08	0.34	1.26	8.77	0.00	1.52	0.10	0.01	7.55
K_2O	0.01	0.03	1.34	9.61	0.28	0.00	0.93	9.08	0.01	0.05	0.00	0.00	8.64	8.89	0.05	0.00	0.80	8.61	0.01	0.08
Total	100.65	98.89	96.04	94.56	100.19	100.13	94.71	91.74	96.59	100.10	100.62	95.17	95.32	95.52	100.12	98.99	96.19	92.49	99.43	99.13
Ox.	12	6	24	22	8	12	24	22	12.5	8	12	48	22	22	8	12	24	22	12.5	8
Si	2.992	1.933	6.412	5.534	2.789	2.983	6.368	5.501	3.049	2.710	2.980	8.105	5.522	6.143	2.734	2.982	6.607	5.575	3.109	2.661
Ti	0.003	0.007	0.099	0.526	0.000	0.002	0.105	0.256	0.006	0.000	0.001	0.133	0.183	0.086	0.000	0.002	0.094	0.283	0.009	0.002
Al	1.961	0.208	2.781	2.676	1.220	1.967	2.751	3.057	2.420	1.284	1.998	18.480	3.173	5.493	1.265	2.006	2.872	3.091	2.071	1.341
Cr	0.001	0.001	0.004	0.000	0.001	0.002	0.000	0.000	0.003	0.000	0.004	0.007	0.002	0.001	0.000	0.000	0.006	0.001	0.001	0.002
Fe^{2+}	1.539	0.217	1.919	1.762	0.000	1.681	2.124	2.091	0.683	0.003	2.043	2.797	1.646	0.115	0.001	1.806	1.649	1.977	1.662	0.000
Mn	0.031	0.000	0.016	0.004	0.000	0.311	0.056	0.036	0.025	0.000	0.030	0.010	0.004	0.000	0.001	0.065	0.011	0.012	0.105	0.000
Mg	0.860	0.676	2.492	3.150	0.000	0.564	2.418	2.835	0.000	0.000	0.748	0.960	3.316	0.279	0.000	0.461	2.421	2.790	0.372	0.000
Ca	0.635	0.851	1.981	0.006	0.204	0.519	1.951	0.013	2.046	0.292	0.213	0.003	0.005	0.000	0.254	0.690	1.892	0.010	1.017	0.327
Na	0.004	0.126	0.516	0.044	0.755	0.003	0.565	0.039	0.002	0.714	0.005	0.046	0.097	0.322	0.754	0.000	0.457	0.030	0.002	0.657
K	0.001	0.001	0.271	1.841	0.016	0.000	0.192	1.809	0.001	0.003	0.000	0.000	1.616	1.494	0.003	0.000	0.158	1.683	0.001	0.005
Sum	8.027	4.020	16.490	15.544	4.986	8.032	16.530	15.638	8.234	5.007	8.021	30.541	15.564	13.932	5.011	8.012	16.167	15.452	8.348	4.996

Table 4. Results of mineral geothermobarometry on WFO and ortho- and paragneiss from George and Doubtful Sounds. Co-existing rim compositions have been used in *P–T* estimates. Assumed pressures and temperatures are based on best-fit results from average *P–T* calculations using THERMOCALC, where these were able to be calculated.

Sample	Unit	Assemblage	Timing	Assumed P (kbar)	Temperature (°C)	Assumed T (°C)	Pressure (kbar)	Method
Doubtful Sound								
DS08C	WFO	Grt–cpx–hbl–bt–pl–qtz–ilm–rt	$S2^{DS}$	11.3	867 ± 88, 659, 860, 874, 769, 750, 723, 777			1, 2, 3, 4, 5, 6, 7, 8
						877	11.3 ± 1.2, 11.9, 13.0, 12.7, 10.7	1, 11, 12, 13, 14
DS49A	WFO	Grt–cpx–hbl–pl–qtz–ilm–rt	$S2^{DS}$	11.3	933, 842, 824, 800, 866			4, 5, 6, 7, 8
						877	10.2, 11.6, 11.5, 9.6	11, 12, 13, 14
DS40C	P/G	Grt–hbl–bt–czo–pl–qtz	$S2^{DS}$	10.6	629 ± 18, 695			1, 4
						628	10.6 ± 0.6, 9.5, 10.0	1, 11, 12
DS67	O/G	Grt–bt–czo–pl–qtz	$S2^{DS}$	13.3	650 ± 18, 548, 683			1, 2, 3
						651	13.3 ± 1.3	1
George Sound								
GS9717B	P/G	Grt–st–bt–ms–ky–pl–qtz	$S1^{GS}$	8.4	654 ± 9, 571, 597			1, 2, 3
						655	8.4 ± 0.6, 9.0, 9.0	1, 12, 10
GS9714C	P/G	Grt–st–bt–ms–ky–pl–qtz	$S1^{GS}$	9.0	660 ± 17, 638, 752			1, 2, 3
						662	8.9 ± 1.0, 11.7, 11.7	1, 9, 10
GS9705B	P/G	Grt–hbl–bt–ep–pl–qtz	$S2^{GS}$	12.4	694 ± 43, 664, 906, 735			1, 2, 3, 4
						706	12.3 ± 1.1, 10.9, 10.4	1, 11, 12
GS9705C	P/G	Grt–hbl–bt–czo–pl–qtz–ilm–spn	$S2^{GS}$	11.8	628 ± 13, 691, 949, 632			1, 2, 3, 4
						628	11.8 ± 0.5, 9.6, 9.1	1, 11, 12

Abbreviations: *Internally consistent dataset*: 1 – Holland & Powell (1998), *Thermometers*: 2 – Perchuk & Lavrent'eva (1990); 3 – Ferry & Spear (1978); 4 – Graham & Powell (1984); 5 – Ellis & Green (1979); 6 – Powell (1985); 7 – Krogh (1988); 8 – Berman *et al.* (1995), *Barometers*: 9 – Newton & Haselton (1981); 10 – Koziol & Newton (1988); 11 – Kohn & Spear (1990; Fe); 12 - Kohn & Spear (1990; Me); 13 – Eckert *et al.* (1991; Mg); 14 – Newton & Perkins (1982; Mg). *Thermometers*: G–bt: 2,3, Gt–hbl: 4, Gt–cpx: 5–8, *Barometers*: Grt–als–pl–qtz: 9, 10, Gt–hbl–pl–qtz: 11, 12, Grt–cpx–pl–qtz: 13, 14.

determined using the method of Cawthorn & Collerson (1974).

Mineral chemistry

Doubtful Sound WFO

Coarse-grained plagioclase laths of composition Ab_{70-85} ($Ab = 100\times Na/[K + Ca + Na]$) occur in $S2^{DS}$ assemblages in dioritic and gabbroic WFO at Doubtful Sound. Some are zoned from calcic cores to more sodic rims. In garnet reaction zones plagioclase are usually slightly more calcic than in the host rock (Ab_{65}). K-feldspar in primary assemblages and in garnet-bearing veins is almost pure orthoclase, $Or_{87-100}An_{0-12}Ab_{0-1}$ ($Or = 100\times K/[K + Ca + Na]$, $An = Ca/[K + Ca + Na]$). Rare igneous orthopyroxene shows no growth zonation and has the general composition $En_{55}Fs_{45}$. With proximity to garnet reaction zones orthopyroxene becomes more enriched in Al^{4+} and depleted in Fe^{2+}. The general composition of relict igneous clinopyroxene is $Woll_{40}En_{33}Fs_{10}Jd_{12}$-$CaTs_5$. Metamorphic clinopyroxene, common in garnet reaction zones and garnet-bearing trondjemitic veins, is more variable in composition. It is depleted in Fe^{2+} and enriched in Na and Al^{4+} relative to igneous clinopyroxene, typically $Woll_{38-40}En_{33-39}Fs_{8-14}$ Jd_{14-24}. In garnet reaction zones recrystallized during development of Doubtful Sound shear zone fabrics ($S2^{DS}$), metamorphic clinopyroxene shows depletion in Na and enrichment in Ca and Mg ($Woll_{41-46}En_{37-38}$ Fs_8Jd_{9-12}). Garnet occurs in three textural and mineralogical settings within the WFO: in trondjemitic veins; in garnet reaction zones and static pseudomorphs of hornblende in scattered localities; and in later shear-fabrics. At Doubtful Sound garnet in reaction zone assemblages fall in the range $Alm_{40-50}Grs_{10-22}Prp_{30-40}Sps_{0-1}$ ($Alm = 100\times Fe^{2+}/[Fe^{2+} + Mg + Ca + Mn + Fe^{3+}]$, $Grs = 100 \times Ca/[Fe^{2+} + Mg + Ca + Mn + Fe^{3+}]$, $Prp = 100 \times Mg/[Fe^{2+} + Mg + Ca + Mn + Fe^{3+}]$, $Sps = 100 \times Mn/[Fe^{2+} + Mg + Ca + Mn + Fe^{3+}]$). Garnet recrystallized during later shear associated with formation of the Doubtful Sound shear zone ($S2^{DS}$) shows a slight enrichment in Fe/Mg, typically $Alm_{45-55}Grs_{10-20}$ $Prp_{25-35}Sps_1$. Amphibole ($S2^{DS}$) is pargasitic with $XMg = 0.5–0.69$ ($XMg = Mg/[Mg + Fe^{2+}]$). Biotite ($S2^{DS}$) has $XMg = 0.6–0.75$ and is rich in Ti: 0.35–0.53 cations per formula unit (f.u.).

Doubtful Sound paragneiss and interleaved orthogneiss

Plagioclase varies widely in composition in ortho- and paragneiss from within the regional gneiss sequence at Doubtful Sound. Plagioclase in paragneiss units and calc-silicates fall in the range Ab_{54-72}. Plagioclase in orthogneiss units interleaved with paragneiss is more sodic, Ab_{66-75}, some showing a core to rim increase in sodium content. The most sodic plagioclase is found in post-$D2^{DS}$ felsic veins containing peritectic garnet, Ab_{80-98}. Garnet occurs as a porphyroblastic phase in paragneiss and interleaved orthogneiss. $S2^{DS}$ garnet from paragneiss at Doubtful Sound is typically more Mg-rich and/or Ca-poor than in $S2^{GS}$ in the GSP: $Alm_{46-50}Grs_{14-21}Prp_{28-31}Sps_{0-1}$. They show strong core to rim zonation characterized by increasing Ca and decreasing Mg. Some paragneiss has unusually Mn-rich garnet: $Alm_{50-54}Grs_{7-16}Prp_{15-23}Sps_{10-12}$, as

does garnet in some interleaved orthogneiss units: $Alm_{47-55}Grs_{23-27}Prp_{11-13}Sps_{6-13}$. Amphibole in $S2^{DS}$ fabrics in the paragneiss is pargasitic (XMg = 0.55–0.65). Amphibole from interleaved orthogneiss has generally higher XMg but are otherwise similar in composition to that in the paragneiss. Biotite from Doubtful Sound paragneiss ($S2^{DS}$) falls in the range XMg = 0.57–0.68 and 0.26–0.37 Ti cations per f.u. Biotite from interleaved orthogneiss ($S2^{DS}$) has XMg 0.46–0.53 and 0.17–0.3 Ti cations per f.u. Epidote group minerals are common in para- and orthogneiss at Doubtful Sound, in which it is texturally and chemically indistinguishable, with Czo_{37-45} [Czo = $100 \times (Al\text{-}2)/(Al\text{-}2 + Fe^{3+})$].

George Sound paragneiss

Feldspar in the GSP is almost entirely plagioclase though K-feldspar is present in the migmatitic contact zone (Degeling, 1997). In $S1^{GS}$ assemblages plagioclase is typically in the range Ab_{73-77} and in diatexic GSP and post-$D2^{GS}$ garnet-bearing felsic veins it falls in the range Ab_{60-70}. $S1^{GS}$ garnet porphyroblasts in the GSP, typically $Alm_{65-68}Grs_{3-7}Prp25\text{-}_{31}Sps_1$, show chemical zonation characterized by increasing Ca and Fe content from core to rim. $S2^{GS}$ garnet is enriched in Ca relative to $S1^{GS}$ garnet ($Alm_{60-62}Grs_{19-23}Prp_{14-16}Sps_{1-2}$). Garnet in calc-schists is very grossular-rich ($Alm_{49}Grs_{34}Prp_{11}Sps_3$), some showing a rimward decrease in grossular content. Garnet in the diatexic paragneiss from the GSP forms fine-grained rims around amphibole and plagioclase. Although otherwise compositionally similar it has a higher spessartine content than typical $S2^{GS}$ garnet ($Alm_{50-53}Grs_{18-22}Prp_{16-22}Sps_{6-9}$). Peritectic garnet associated with post-$S2^{GS}$ felsic veins is unzoned and also compositionally similar to $S2^{GS}$ garnet ($Alm_{57}Grs_{18}Prp_{21}Sps_2$). Amphibole is restricted to $S2^{GS}$ and is pargasitic in composition (XMg = 0.54–0.62). Biotite in $S1^{GS}$ assemblages in the GSP has XMg = 0.62–0.67 and typically 0.18 Ti cations per f.u. In $S2^{GS}$ assemblages biotite is more Fe and Ti rich: XMg = 0.57–0.6 and 0.29 Ti cations per f.u. White mica in $S1^{GS}$ and $S2^{GS}$ assemblages is muscovite-rich with XK = 0.82–0.94 (XK = K/[K + Na]) with a phengitic component of 0.3–0.7 Fe^{2+} + Mg cations on the octahedral site. Epidote group minerals are common in paragneiss in the GSP. Epidote in $S1^{GS}$ assemblages in the GSP has Czo_{40}. In $S2^{GS}$ assemblages it is more clinozoisite-rich (Czo_{75}). Clinozoisite is also associated with later metasomatism throughout the GSP (Czo_{62-75} and $_{75-91}$ in calc-schists). Rare staurolite in the GSP is Fe-rich (XMg = 0.2–0.26).

Thermobarometry

Emplacement of the WFO (stage 1) has been constrained to *c.* < 8 kbar and > 750 °C, on the basis of occurrence of two pyroxene-bearing S1 assemblages (e.g. Clarke *et al.*, 2000). Data from Daczko *et al.* (2002b)) give *P–T* estimates of *c.* 12 kbar and 700–750 °C for the development of garnet reaction zones (stage 2) in the ARC, near the intrusive contact of the WFO at Mt Daniel. In Doubtful Sound garnet-bearing $S2^{DS}$ assemblages from the WFO within and adjacent to the Doubtful Sound shear zone (led to stage 4) give estimates of 750–850 °C and 10–13 kbar (DS08C and DS49A). This is consistent with the estimates of garnet reaction zone formation from Mt Daniel. Para- and orthogneiss within the shear zone at Kellard Point give estimates of *c.* 600–700 °C and 10–13 kbar (DS67). This is consistent with the WFO and adjacent para- and orthogneissic rocks having occupied similar crustal depths. The higher temperatures recorded by the WFO compared with the para- and orthogneissic rocks may be a consequence of systematic error; i.e. the lower temperatures are given by garnet–hornblende and garnet–biotite, and the higher temperatures by garnet–clinopyroxene thermometry.

No pressure or temperature estimates are available for the WFO from George Sound as these rocks are not garnet-bearing. However, they do contain relict igneous and early metamorphic two pyroxene-bearing assemblages indicative of early low-pressure during emplacement (stage 1; *c.* < 8 kbar; Degeling, 1997). Early low-pressure conditions are consistent pressure estimates from low strain zones within the GSP (see also Daczko *et al.*, 2002a). Samples from within these low strain zones preserve $S1^{GS}$ assemblages that predate intrusion of the WFO (pre-stage 1). These give estimates of *c.* 600–750 °C and 8–12 kbar (GS9717B and GS9714C). $S2^{GS}$ assemblages from migmatitic and diatexic paragneiss (stage 2 or 3) give similar estimates of *c.* 630–690 °C and 9–12 kbar (GS9705B and GS9705C).

DISCUSSION

Here the three main issues set out in the Introduction are addressed: (i) the timing of emplacement, deformation, and metamorphism of the WFO, (ii) the timing of development of metamorphic assemblages in central and northern Fiordland in general, and (iii) the nature of the crust into which the WFO was emplaced.

Timing of emplacement, deformation, and metamorphism of the WFO

The timing of the emplacement of the WFO cannot be addressed without referring to the geochemically identical and upper crustal level intrusions of the Separation Point Suite. The consanguinity of WFO and Separation Point Suite has been addressed by Muir *et al.* (1998). These rocks have adakitic affinities probably related to the subduction of the Median Tectonic Zone (Muir *et al.*, 1998). Geochronology of Separation Point Suite plutons in the Nelson area range from 119 to 114 Ma (Muir *et al.*, 1994, 1996), while in eastern Fiordland ages of 123–120 Ma are

prevalent (Muir *et al.*, 1998). These age ranges are identical to those determined for WFO samples (Mattinson *et al.*, 1986; McCulloch *et al.*, 1987; Gibson *et al.*, 1988; data presented here) and therefore it is clear that the igneous emplacement age is identical to the age of the metamorphic rocks derived there from.

WFO samples from Mt Daniel, Doubtful Sound and George Sound show a consistency in zircon morphology and U–Pb age data. Zircon from an homogeneous dioritic gneiss (DAN24) and a post-$S1^{MD}$ trondjemitic dyke (DAN23) from Mt Daniel, and from dioritic gneiss samples from Doubtful (CA90) and George Sounds (9710D) show similar relatively homogeneous CL responses with or without fir-tree or patchy sector zonation and in some cases remnant weak oscillatory zonation. On the basis of the consistency in ages (121.8 ± 1.7, 123.6 ± 3.0, 115.6 ± 2.4, and 120.0 ± 2.6 Ma, respectively) and the lack of any inherited grains or cores in these four samples, the ages are interpreted as emplacement ages for the WFO at these localities (stage 1 as defined above). These ages agree with existing geochronological data that place WFO emplacement at 126–116 Ma (Mattinson *et al.*, 1986; McCulloch *et al.*, 1987; Gibson *et al.*, 1988). Chronologically distinct ages from Mt Daniel and Doubtful Sound in this study support the inference of Bradshaw (1990) that the WFO is a composite intrusion made up of distinct intrusive bodies. Bradshaw's further supposition that the WFO was emplaced during deformation is supported by our age data for the dioritic massive gneiss and the post-$D1^{MD}$ trondjemitic dyke at Mt Daniel, which give ages within error of each other (121.8 ± 1.7 and 123.6 ± 3.0 Ma, respectively). The age of this dyke constrains the earliest phase of deformation recorded in the WFO from this area – $S1^{MD}$, possibly a reworked magmatic foliation – developed prior to or during burial to conditions of *c.* 12 kbar and 700–750 °C (e.g. Daczko *et al.*, 2002b; stages 1–2). Similarly Muir *et al.* (1995) reported an emplacement age of 125.9 ± 1.9 Ma for a sample of the WFO west of Lake Quill in the Franklin Mountains (within 4 km of Mt Daniel), again within error of the post-$D1^{MD}$ dyke. In George Sound the same conclusion is supported by the occurrence of Cretaceous rims on detrital zircon cores within $S2^{GS}$ metamorphic assemblages in the GSP. On the basis of the clustering of data around *c.* 117 Ma in sample 9713A, on the morphology of the rims (Fig. 2), and the tendency toward lower Th/U these are interpreted as metamorphic rims formed during development of the dominant $S2^{GS}$ assemblages in these rocks (Table 1; stages 1–2). As $S2^{GS}$ affected both the WFO and the GSP, $D2^{GS}$ is considered to have occurred synchronous with WFO emplacement in George Sound.

The development of garnet reaction zones in the WFO has previously been cited as evidence for high-pressure metamorphic conditions of *c.* 700–800 °C and *c.* 12–14 kbar during their formation (Bradshaw, 1985, 1989a, 1990; Clarke *et al.*, 2000; Daczko *et al.*, 2001a,b). These garnet reaction zones are found at Mt Daniel, Doubtful Sound, Poison Bay and in the Pembroke Valley (Fig. 1). Early two pyroxene-bearing assemblages have been described which are attributed to early low-pressure conditions of <8 kbar at >750 °C (Clarke *et al.*, 2000; Daczko *et al.*, 2002a). Thus the occurrence of garnet reaction zones implies a significant increase in pressure conditions prior to their formation. However, ARC mineral assemblages from within the contact aureole adjacent to the WFO at Mt Daniel preserve only high-pressure conditions of 12–14 kbar (e.g. Daczko *et al.*, 2002b). It may be that prolonged magmatic activity at this locality erased any evidence of the earlier history within the contact aureole rocks. A model involving prolonged magmatic activity at the base of the WFO pluton is supported by the isolated complexity of inheritance at the WFO margin at Mt Daniel. Zircon from a garnet reaction zone within the WFO at Doubtful Sound was dated to try to constrain the timing of garnet reaction zone formation. The zircon shows the same morphological features as those from a granoblastic dioritic WFO sample from the same locality and the two also give ages within error (114.0 ± 2.2 and 115.6 ± 2.4 Ma, respectively). This is interpreted as being indicative of no zircon recrystallization or new growth during garnet reaction zone formation (stage 2).

In fact, in no case has any WFO sample been found where early Cretaceous zircon (*c.* 126 Ma) has been superposed by metamorphic zircon that correlates with a later phase of WFO emplacement (e.g. *c.* 114 Ma), despite the fact that such early Cretaceous rims on zircon are well-developed in some paragneiss samples: Essentially, all samples of SPS and WFO that have been analyzed by SHRIMP, with accompanying CL, show single formation events and no subsequent overprint that could be ascribed to a metamorphic event. These observations support the supposition of Hollis *et al.* (2003) that metamorphism of Cretaceous magmas may be the product of autometamorphism.

Timing of development of metamorphic assemblages in central and northern Fiordland

At Mt Daniel the *c.* 123 Ma WFO was emplaced into the only marginally older (*c.* 129 Ma; Hollis *et al.*, 2003) dioritic to gabbroic ARC, generating partial melting of the ARC and a well-developed contact aureole. The ARC is considered to have formed as the final phase of magmatism associated with the Median Tectonic Zone in an island arc setting (Hollis *et al.*, 2003). Emplacement of the WFO into these rocks and burial of the terrane, evidenced by the generation of high-pressure garnet reaction zones, are consistent with the early Cretaceous arc-continent collision model (Bradshaw, 1985, 1989a; Clarke *et al.*, 2000; Daczko *et al.*, 2001a,b, 2002a,c). Amphibolite to granulite facies metamorphic assemblages were almost certainly developed synchronously in the WFO and ARC in

northern Fiordland on the basis that (1) the WFO and ARC preserve evidence for a similar burial history (development of garnet reaction zones post-dating early two pyroxene-bearing assemblages) and (2) rare *c*. 120 Ma metamorphic rims on older Cretaceous (*c*. 134 Ma) zircon have been identified in the ARC (Tulloch *et al*., 2000), consistent with amphibolite to granulite facies metamorphism of the ARC during emplacement of the WFO (stage 1).

At Doubtful and George Sounds there is considerable evidence in the zircon data that the thermal pulse associated with WFO emplacement was responsible for the generation of the amphibolite to granulite facies assemblages recorded in the regional gneiss. From Kellard Point in Doubtful Sound we have dated a strongly foliated paragneiss that holds an amphibolite facies $S2^{DS}$ assemblage (Table 1). Nine CL-homogeneous small grains and rims on oscillatory-zoned grains are interpreted as metamorphic in origin on the basis of their morphology (Fig. 2), a tendency toward low Th/U (typically <0.2), and a combined age of 117.7 ± 2.8 Ma. Excess dispersion in the spread of ages, consistent with the results from depth profiles through the rims of three grains, suggest that two phases of early Cretaceous metamorphism may have affected these rocks. This is consistent with results of Gibson *et al*. (1988), who reported significant spread in the age data from a Cretaceous amphibolite facies mylonite from within the strongly sheared margin between the WFO and Palaeozoic metasedimentary sequence at Doubtful Sound (127–109 Ma). However, in both data sets distinct metamorphic episodes are not resolvable with the available data. Also, only a single phase of metamorphism is preserved in the metamorphic mineral assemblage in sample ($S2^{DS}$). We interpret the 117.7 ± 2.8 Ma age as the age of the $S2^{DS}$ assemblage in this sample. Thermobarometry on ortho- and paragneiss samples from the same locality (DS40C, DS67; Table 4) give *P–T* estimates of 600–700 °C and 10–13 kbar for $S2^{DS}$. The age of this metamorphism falls within error of the emplacement age of the tectonically juxtaposed WFO in Doubtful Sound (i.e. 115.6 ± 2.4 Ma) consistent with the generation of amphibolite facies metamorphic assemblages associated with the thermal effect of WFO emplacement (stage 1). Furthermore, *P–T* estimates for $S2^{DS}$ assemblages in ortho- and paragneiss samples from within the Doubtful Sound shear zone (*c*. 600–700 °C and 10–13 kbar) and the WFO within and adjacent to the Doubtful Sound shear zone (750–850 °C and 10–13 kbar) are consistent with their having occupied similar crustal depths.

At George Sound a migmatized intrusive contact zone between the WFO and the GSP is well-exposed. The WFO at this locality post-dates amphibolite facies $S1^{GS}$ assemblages in low-strain zones in the GSP, which formed at *c*. 600–750 °C and 8–12 kbar (GS9717B and GS9714C; Table 4; pre-stage 1). Both WFO and GSP hold a variably developed $S2^{GS}$, indicative of $D2^{GS}$ deformation after emplacement of the WFO. An unfoliated amphibolite facies paragneiss (9713A; Table 1) in the migmatized contact zone with the WFO shows strong development in its zircon population of CL-homogeneous small grains and rims on oscillatory-zoned cores (Fig. 2), interpreted as metamorphic in origin on the basis of their morphology and coincidence of age data: 12 analyses yield a weighted mean of 117.2 ± 1.3 Ma (stages 1–2). As is the case at Doubtful Sound, this falls within error of the 120.0 ± 2.6 Ma emplacement age of the WFO at this locality, consistent with the interpretation that generation of $S2^{GS}$ amphibolite facies assemblages in the GSP was induced by intrusion of the WFO. In the GSP amphibolite facies $S2^{GS}$ assemblages formed under conditions of *c*. 630–690 °C and 9–12 kbar (GS9705B and GS9705C).

Temperatures of metamorphism of paragneiss at both Doubtful and George Sounds are lower by *c*. 100 °C than corresponding temperatures derived for metamorphism of the WFO at both Doubtful Sound and Mt Daniel (no temperature data is available for the WFO at George Sound owing to the lack of garnet). The significance of this is difficult to evaluate and may simply be a consequence of systematic error associated with higher temperature estimates from garnet-clinopyroxene thermometers. It does appear, however, that there is a consistency in lower peak pressure estimates from paragneiss samples from George Sound (*c*. 8–12 kbar; see also Daczko *et al*., 2002a) compared with Mt Daniel (*c*. 12 kbar; Daczko *et al*., 2002b) and Doubtful Sound (*c*. 10–13 kbar; Table 1). This suggests that the GSP may not have reached the same crustal depths as other parts of the Fiordland Block during early Cretaceous emplacement of the WFO and collisional orogenesis.

The regional significance of the Cretaceous thermal event in the development of high-grade metamorphic assemblages has been the subject of some debate. The coincidence of WFO emplacement ages with metamorphic age data coupled with *P–T* data (this study and in Daczko *et al*., 2002a) from the three areas indicate that WFO emplacement induced amphibolite to granulite facies metamorphism in host rocks over a wide area of central and northern Fiordland. Although there are some indications of a prolonged or two-stage metamorphic history from the zircon systematics of the Doubtful Sound paragneiss (CA39M; see also Gibson *et al*., 1988) we are only able to confidently chronologically constrain a single metamorphic episode, correlated with emplacement of the WFO. The coincidence of metamorphic ages correlated with high-pressure assemblages and Mt Daniel and Doubtful Sound, and with moderate pressure assemblages at George Sound, suggest that emplacement of the WFO at upper to mid crustal levels and burial of the terrane to mid to deep crustal levels (stages 1 & 2) occurred within a period of only

a few million years: we are unable to resolve these different phases of the tectonometamorphic history in the geochronological data.

There is little doubt from the petrological and age data presented in Ireland & Gibson (1998) that in central and southern Fiordland the current expression of Cretaceous metamorphism is more limited relative to northern Fiordland. Here regional Palaeozoic metamorphic ages are prevalent with Cretaceous metamorphism of paragneiss localized in the region of Cretaceous intrusions. Distal to those intrusions, Palaeozoic metamorphic ages are more prevalent (Ireland & Gibson, 1998). Gibson *et al.* (1988) noted that Ar–Ar loss from Palaeozoic hornblende and biotite associated with a Cretaceous thermal event is more pronounced with proximity to Cretaceous plutons in central Fiordland. It is likely that the apparent difference in metamorphic response in central and southern compared with northern Fiordland is the product of excision of intrusive WFO exposure and of significant thicknesses of once adjacent ortho- and paragneiss in central Fiordland via tectonic thinning: evidence of post-WFO extension is widespread in central Fiordland (see also Gibson *et al.*, 1988).

Nature of the crust into which the WFO was emplaced

Field relationships coupled with geochronology data support a tectonic model involving emplacement of the WFO during collision of the Mesozoic MTZ arc with the Palaeo-Pacific Gondwana margin (see also Clarke *et al.*, 2000; Daczko *et al.*, 2001a,b, 2002a,b,c). The WFO shows intrusional relationships with the 136–129 Ma ARC in northern Fiordland (the product of late-stage MTZ magmatism), which in turn shows evidence for emplacement into Palaeozoic orthogneiss (Hollis *et al.*, 2003). Age relationships for one of the WFO samples from Mt Daniel show more complexity than the four simple early Cretaceous emplacement ages reported here (see discussion above). A dioritic WFO gneiss (DAN22) preserves only inherited zircon grains, a few with Cretaceous metamorphic rims consistent with the emplacement age of the main body of the WFO (DAN24; 121.8 ± 1.7 Ma). The post-$D1^{MD}$ dyke (DAN23) also shows some evidence for an inherited component. These samples are significant in that they illustrate that the WFO plutons at this locality sampled older continental material. Inheritance of this kind has not been observed in other geochronological studies of the WFO. This inheritance is consistent with partial melting of old Western Province sedimentary material that may have been subducted during the final stages of collisional orogenesis, or assimilation of wall rock material around the magma chambers.

In Doubtful Sound the contact between the WFO and the regional ortho- and paragneiss sequence is strongly tectonized along the Doubtful Sound shear zone. However zircon data are consistent with (at least localized) metamorphism of the central Fiordland paragneiss sequence during emplacement of the WFO at *c.* 117 Ma. Detrital zircon from a paragneiss at Kellard Point in Doubtful Sound show Pacific Gondwana age spectra, i.e. dominant peaks at 1700, 1100–1000 and 600–500 Ma, and with a minor Archean component (*cf.* Ireland, 1992; Wysoczanski *et al.*, 1997; Ireland & Gibson, 1998). The youngest detrital cores indicate a maximum depositional age in the Devonian. These results are consistent with similar age spectra and depositional ages for sedimentary rocks of the Lachlan Fold Belt (Williams *et al.*, 1992), and paragneiss from Fiordland and Westland (Fraser Formation, Greenland Group; Ireland, 1992; Ireland & Gibson, 1998), Northern Victoria Land and Marie Byrd Land (Adams, 1987; Weaver *et al.*, 1991; Cooper & Tulloch, 1992; Ireland *et al.*, 1994; Fergusson & Fanning, 2002). Coupled with the remarkably similar record of mid-Palaeozoic and Mesozoic magmatism in the Western Province of New Zealand, the Lachlan Fold Belt, the central Queensland coast, Northern Victoria Land and Marie Byrd Land, this supports arguments for the contiguity of these regions in the Mesozoic, and the derivation of sedimentary precursors of Fiordland and Nelson-Westland paragneiss and sedimentary rocks of the Lachlan Fold Belt from the same sources.

The Permo-Triassic zircon populations in the GSP set it apart from the much older paragneiss units previously studied in Fiordland. The interpretation of the GSP data are not straightforward because of potential resetting of zircon U–Pb systematics from the emplacement of the WFO. Nevertheless, zircon age spectra from Palaeozoic sedimentary precursors are readily recognizable as similar to the Gondwana greywacke signature (Ireland & Gibson, 1998). The GSP spectra are quite distinct from this. The coincidence of ages, especially in sample 9705 where 11 of the 23 analyses comprise two groups, suggests that the zircon are derived from a Permo-Triassic source. The effects of Cretaceous resetting would be to smear out the detrital age signature, not to cause homogeneous Pb loss in several zircon with differing U and Th concentrations. Furthermore, individual zircon have differing propensity for microfracturing, this being the main channel for Pb loss, relating to the microstructure and environment of the individual zircon. It is thus likely, as in the case of the Palaeozoic sedimentary source, that the detrital zircon signature reflects, at least in part, the source provenance.

The presence of a Permo-Triassic sedimentary component in Fiordland has not been described previously. However, such a signature has been found in the Western Province. Wysoczanski *et al.* (1997) reported such an occurrence from Parapara Peak in the Takaka Terrane of Westland (*c.* 240 Ma). Here the detrital zircon age spectra consist of mixtures of both Permo-Triassic and Gondwana-signature zircon. This

spectrum is thus identical in components to zircon ages from the Torlesse terrane of the Eastern Province indicating the distinctions between Western and Eastern Provinces are not as profound as originally proposed. Indeed the contribution of Mesozoic and also Proterozoic to Archean sources may be indicative of the close proximity of the Eastern and Western Provinces by the late Jurassic. This is supported by the early Cretaceous ages of ARC orthogneiss (136–129 Ma), interpreted as the last phase of MTZ plutonism, emplaced into the Western Province and similarly aged intrusives in Westland (Muir *et al*., 1997; Hollis *et al*., 2003).

A Permo-Triassic depositional age for at least part of the GSP constrains development of metamorphic assemblages to Cretaceous rather than an alternative possibility in the Palaeozoic. Furthermore the age data provides support for a model involving crustal thickening during and/or after WFO emplacement, requiring burial of the GSP from the surface to al least 25 km depth by *c*. 120 Ma.

CONCLUSIONS

U–Pb SHRIMP zircon age data shows that the western Fiordland Orthogneiss was emplaced as a series of plutons in the early Cretaceous. Emplacement during regional deformation is supported by (i) synchronous ages of host WFO and a WFO dyke that post-dates early deformation at Mt Daniel and (ii) the Cretaceous metamorphism and deformation of paragneiss in George and Doubtful Sounds. Intrusional field relationships at George Sound and Mt Daniel and the development of Cretaceous metamorphic zircon in paragneiss from George and Doubtful Sounds indicate that the WFO provided the heat source for amphibolite–granulite facies metamorphism in central and northern Fiordland. In central Fiordland the extent of the metamorphic effects of WFO emplacement is limited to the immediate vicinity of Cretaceous plutons: the dominant metamorphic assemblages reflect Palaeozoic thermal events. However, orthogneiss (ARC) and paragneiss (GSP) in northern Fiordland preserve Cretaceous metamorphic assemblages associated with the emplacement of the WFO. A sample of paragneiss from Doubtful Sound has a Pacific Gondwana age spectra with peaks at 1700, 1100–900 and 600–500 and a small Archean component, with a maximum depositional age in the Devonian. Three samples of the GSP may be much younger, with source components of likely Permo-Triassic age. This would limit the development of moderate to high-pressure amphibolite to granulite facies mineral assemblages in the GSP to the Cretaceous. These data support existing petrological, thermobarometric, and structural evidence for collisional crustal thickening of the Mesozoic Pacific Gondwana margin during early Cretaceous emplacement of the WFO.

ACKNOWLEDGEMENTS

JAH field and analytical work were supported by an Australian Research Council grants to G.L.C. and K.A.K. (A10009053, DP0342862) and National Science Foundation funding to KAK (EAR-0087323). J. Stevenson, J. Fitzherbert, F. Schröter, and M. Baker assisted in collecting SHRIMP analyses. H. Degeling, J. Stevenson, and J. Harnmeijer carried out some of the field work and microprobe analyses. S. Weaver, J. Herman and D. Rubatto are thanked for constructive and thorough reviews.

SUPPLEMENTARY MATERIAL

The following material is available from http://www.blackwellpublishing.com/products/journals/suppmat/jmg/jmg537/jmg537sm.htm

Table S1. Zircon U–Pb SHRIMP data. Rims around oscillatory-zoned cores, or small grains with homogeneous CL response in dominantly oscillatory-zoned zircon populations are interpreted as metamorphic zircon. Analyses of these are marked with an asterisk. The values given in the AGE column are ^{207}Pb-corrected ^{238}U/^{206}Pb ages except for paragneiss samples CA39M and 9717B where they are the ^{204}Pb-corrected inferred age based on weighted mean ^{238}U/^{206}Pb and ^{207}Pb/^{206}Pb ages.

REFERENCES

Adams, C. J., 1987. Geochronology of granite terranes in the Ford Ranges, Marie Byrd Land, West Antarctica. *New Zealand Journal of Geology and Geophysics*, **30,** 51–72.

Adams, C. J., Barley, M. E., Maas, R. & Doyle, M. G., 2002. Provenance of Permian-Triassic volcanoclastic sedimentary terranes in New Zealand: evidence from their radiogenic isotope characteristics and detrital mineral age patterns. *New Zealand Journal of Geology and Geophysics*, **45,** 221–242.

Berman, R. G., Aranovich, L. Y. & Pattison, D. R. M., 1995. Reassessment of the garnet–clinopyroxene Fe–Mg exchange thermometer: II. Thermodynamic analysis. *Contributions to Mineralogy and Petrology*, **119,** 30–42.

Borg, S. G., Stump, E., Chappell, B. W. *et al*., 1987. Granitoids of northern Victoria Land, Antarctica; implications of chemical and isotopic variations to regional crustal structure and tectonics. *American Journal of Science*, **287,** 127–169.

Bradshaw, J. Y., 1985. *Geology of the Northern Franklin Mountains, Northern Fiordland, New Zealand, with Emphasis on the Origin and Evolution of Fiordland Granulites*. Unpublished Ph.D. Thesis. University of Otago, Dunedin, New Zealand.

Bradshaw, J. D., 1989a. Cretaceous geotectonic patterns in the New Zealand region. *Tectonics*, **8/4,** 803–820.

Bradshaw, J. Y., 1989b. Origin and metamorphic history of an early Cretaceous polybaric granulite terrain, Fiordland, southwest New Zealand. *Contributions to Mineralogy and Petrology*, **103,** 346–360.

Bradshaw, J. Y., 1990. Geology of crystalline rocks of northern Fiordland: details of the granulite facies western Fiordland Orthogneiss and associated rocks. *New Zealand Journal of Geology and Geophysics*, **33,** 465–484.

Bradshaw, J. D., 1993. A review of the Median Tectonic Zone: terrane boundaries and terrane amalgamation near the

Median Tectonic Line. *New Zealand Journal of Geology and Geophysics*, **36,** 117–125.
Bradshaw, J. Y. & Kimbrough, D. L., 1991. Mid-Paleozoic age of granitoids in enclaves within early Cretaceous granulites, Fiordland, southwest New Zealand. *New Zealand Journal of Geology and Geophysics*, **34,** 455–469.
Brown, E. H., 1996. High-pressure metamorphism caused by magma loading in Fiordland, New Zealand. *Journal of Metamorphic Geology*, **14,** 441–452.
Cawthorn, R. G. & Collerson, K. D., 1974. The recalculation of pyroxene end-member parameters and the estimation of ferrous and ferric iron content from electron microprobe analyses. *American Mineralogist*, **59,** 1203–1208.
Chappell, B. W. & White, A. J. R., 1992. I- and S-type granites in the Lachlan fold belt. *Geological Society of America*, **272,** 1–26.
Clarke, G. L., Klepeis, K. A. & Daczko, N. R., 2000. Cretaceous high-P granulites at Milford Sound, New Zealand: metamorphic history and emplacement in a convergent margin setting. *Journal of Metamorphic Geology*, **18,** 359–374.
Cooper, R. A. & Tulloch, A. J., 1992. Early Palaeozoic terranes in New Zealand and their relationship to the Lachlan fold belt. *Tectonophysics*, **214,** 129–144.
Cumming, G. L. & Richards, J. R., 1975. Ore lead isotope ratios in a continuously changing Earth. *Earth and Planetary Science Letters*, **28,** 155–171.
Daczko, N. R., Klepeis, K. A. & Clarke, G. L., 2001a. Evidence of early Cretaceous collisional-style orogenesis in northern Fiordland, New Zealand and its effects on the evolution of the lower crust. *Journal of Structural Geology*, **23,** 693–713.
Daczko, N. R., Clarke, G. L. & Klepeis, K. A., 2001b. Transformation of two-pyroxene hornblende granulite to garnet granulite involving simultaneous melting and fracturing of the lower crust, Fiordland, New Zealand. *Journal of Metamorphic Geology*, **19,** 547–560.
Daczko, N. R., Clarke, G. L. & Klepeis, K. A., 2002a. Thermomechanical evolution of the crust during convergence and mid-crustal pluton emplacement in the Western Province of Fiordland, New Zealand. *Tectonics*, **21,** 10.1029/2001TC001282.
Daczko, N. R., Stevenson, J. A., Clarke, G. L. & Klepeis, K. A., 2002b. Successive hydration and dehydration of high-P mafic granofels involving clinopyroxene–kyanite symplectites, Mt Daniel, Fiordland, New Zealand. *Journal of Metamorphic Geology*, **20,** 669–682.
Daczko, N. R., Clarke, G. L. & Klepeis, K. A. 2002c. Kyanite–paragonite-bearing assemblages, northern Fiordland, New Zealand: rapid cooling of the lower crustal root to a Cretaceous magmatic arc. *Journal of Metamorphic Geology*, **20,** 887–902.
Degeling, H. D., 1997. *Mid-Crustal Response to Syntectonic Pluton Emplacement, George Sound, New Zealand*. Unpublished Honours Thesis. University of Sydney, Sydney, NSW, Australia.
Eckert, J. O., Newton, R. C. & Kleppa, O. J., 1991. The H of reaction and recalibration of garnet–pyroxene–plagioclase–quartz geobarometers in the CMAS system by solution calorimetry. *American Mineralogist*, **76,** 148–160.
Ellis, D. J. & Green, D. H., 1979. An experimental study of the effect of Ca upon garnet–clinopyroxene Fe–Mg exchange equilibria. *Contributions to Mineralogy and Petrology*, **71,** 13–22.
Ewart, A., Schon, R. W. & Chappell, B. W., 1992. *The Cretaceous Volcanic-Plutonic Province of the Central Queensland (Australia) coast – A Rift-Related 'Calc-Alkaline' Province*. Transactions of the Royal Society of Edinburgh, Earth Science, **83,** 327–345.
Fergusson, C. L. & Fanning, C. M., 2002. Late Ordovician stratigraphy, zircon provenance and tectonics, Lachlan Fold Belt, southeastern Australia. *Australian Journal of Earth Sciences*, **49,** 423–436.
Ferry, J. M. & Spear, F. S., 1978. Experimental calibration of the partitioning of Fe and Mg between biotite and garnet. *Contributions to Mineralogy and Petrology*, **66,** 113–117.
Gibson, G. M. & Ireland, T. R., 1995. Granulite formation during continental extension in Fiordland, New Zealand. *Nature*, **375,** 479–482.
Gibson, G. M., McDougall, I. & Ireland, T. R., 1988. Age constraints on metamorphism and the development of a metamorphic core complex in Fiordland, southern New Zealand. *Geology*, **16,** 405–408.
Graham, C. M. & Powell, R., 1984. A garnet-hornblende geothermometer; calibration, testing, and application to the Pelona Schist, Southern California. *Journal of Metamorphic Geology*, **2,** 13–31.
Harnmeijer, J. P., 2001. *A Case for Cretaceous Loading and Exhumation of a Granulite Terrain at Doubtful Sound, Fiordland, New Zealand*. Unpublished Honours Thesis. University of Sydney, Sydney, NSW, Australia.
Holland, T. J. B. & Powell, R., 1998. An internally consistent thermodynamic data set for phases of petrological interest. *Journal of Metamorphic Geology*, **16,** 309–343.
Hollis, J. A., Clarke, G. L., Klepeis, K. A., Daczko, N. R. & Ireland, T. R., 2003. Geochronology and geochemistry of high-pressure granulites of the Arthur River Complex, Fiordland, New Zealand: Cretaceous Magmatism and Metamorphism on the Palaeo-Pacific Margin. *Journal of Metamorphic Geology*, **21,** 299–313.
Ireland, T. R., 1992. Crustal evolution of New Zealand: evidence from age distributions of detrital zircons in Western Province paragneisses and Torlesse greywacke. *Geochimica et Cosmochimica Acta*, **56,** 911–920,
Ireland, T. R. & Gibson, G. M., 1998. SHRIMP monazite and zircon geochronology of high-grade metamorphism in New Zealand. *Journal of Metamorphic Geology*, **16,** 149–167.
Ireland, T. R., Bradshaw, J. Y., Muir, R., Weaver, S. & Adams, C., 1994. Zircon age distributions in granites, greywackes, and gneisses from the Southwest Pacific Gondwana region (Abstracts). *Geological Society of Australia*, **37,** 192–193.
Ireland, T. R., Floettmann, T., Fanning, C. M., Gibson, G. M. & Preiss, W. V., 1998. Development of the early Paleozoic Pacific margin of Gondwana from detrital-zircon ages across the Delamerian Orogen. *Geology*, **26/3,** 243–246.
Kimbrough, D. L. & Tulloch A. J., 1989. Early Cretaceous age of orthogneiss from the Charleston Metamorphic Group, New Zealand. *Earth and Planetary Science Letters*, **95,** 130–140.
Kimbrough, D. L., Mattinson, J. M., Coombs, D. S., Landis, C. A. & Johnston, M. R., 1992. Uranium-lead ages from the Dun Mountain ophiolite belt and Brook Street Terrane, South Island, New Zealand. *Geological Society of America Bulletin*, **104,** 429–443.
Kimbrough, D. L., Tulloch, A. J., Geary, E., Coombs, D. S. & Landis, C. A., 1993. Isotope ages from the Nelson region of South Island, New Zealand: structure and definition of the Median Tectonic Zone. *Tectonophysics*, **225,** 433–448.
Kimbrough, D. L., Tulloch, A. J., Coombs, D. S., Landis, C. A., Johnston, M. R. & Mattinson, J. L., 1994. Uranium-lead zircon ages from the Median Tectonic Zone, New Zealand. *New Zealand Journal of Geology and Geophysics*, **37,** 393–419.
Kohn, M. J. & Spear, F. S., 1990. Two new geobarometers for garnet amphibolites, with applications to southeastern Vermont. *American Mineralogist*, **75,** 89–96.
Koziol, A. M. & Newton, R. C., 1988. Redetermination of the garnet breakdown reaction and improvement of the plagioclase–garnet–Al_2SiO_5–quartz geobarometer. *American Mineralogist*, **73,** 216–223.
Kretz, R., 1983. Symbols for rock-forming minerals. *American Mineralogist*, **68,** 277–279.
Krogh, E. J., 1988. The garnet–clinopyroxene Fe–Mg geothermometer – a reinterpretation of existing experimental data. *Contributions to Mineralogy and Petrology*, **99,** 44–48.

Landis, C. A. & Coombs, D. S., 1967. Metamorphic belts and orogenesis in southern New Zealand. *Tectonophysics*, **4,** 501–518.

Mattinson, J. M., Kimbrough, D. L. & Bradshaw, J. Y., 1986. Western Fiordland Orthogneiss: early Cretaceous arc magmatism and granulite facies metamorphism, New Zealand. *Contributions to Mineralogy and Petrology*, **92,** 383–392.

McCulloch, M. T., Bradshaw, J. Y. & Taylor, S. R., 1987. Sm–Nd and Rb–Sr isotopic and geochemical systematics in Phanerozoic granulites from Fiordland, southwest New Zealand. *Contributions to Mineralogy and Petrology*, **97,** 183–195.

Mortimer, N., Tulloch, A. J., Spark, R. *et al*., 1999. Median batholith and Median Suite of New Zealand: new perspectives on the Phanerozoic igneous record of southern Gondwanaland. *African Journal of Earth Sciences*, **29,** 257–268.

Muir, R. J., Ireland, T. R., Weaver, S. D. & Bradshaw, J. D., 1994. Ion microprobe U–Pb zircon geochronology of granitic magmatism in the Western Province of the South Island, New Zealand. *Chemical Geology (Isotope Geoscience)*, **113,** 171–189.

Muir, R. J., Ireland, T. R., Weaver, S. D., Bradshaw, J. D., Waight, T. E., Jongens, R. & Eby, G. N., 1997. SHRIMP U–Pb geochronology of Cretaceous magmatism in Northwest Nelson, Westland, South Island, New Zealand. *New Zealand Journal of Geology and Geophysics*, **40,** 453–463.

Muir, R. J., Weaver, S. D., Bradshaw, J. D., Eby, G. N. & Evans, J. A., 1995. The Cretaceous Separation Point batholith, New Zealand: granitoid magmas formed by melting of mafic lithosphere. *Journal of the Geological Society of London*, **152,** 689–701.

Muir, R. J., Weaver, S. D., Bradshaw, J. D., Eby, G. N., Evans, J. A. & Ireland, T. R., 1996. Geochemistry of the Karamea Batholith, New Zealand, and comparisons with the Lachlan Fold Belt granites of SE Australia. *Lithos*, **39,** 1–20.

Muir, R. J., Ireland, T. R., Weaver, S. D. *et al*., 1998. Geochronology and geochemistry of a Mesozoic magmatic arc system, Fiordland, New Zealand. *Journal of the Geological Society of London*, **155,** 1037–1053.

Newton, R. C. & Haselton, H. T., 1981. Thermodynamics of the garnet–plagioclase–Al_2SiO_5–quartz geobarometer. In: *Thermodynamics of Minerals and Melts* (eds Newton, R.C., Navrotsky, A. & Wood, B.J.), pp. 131–147, Springer-Verlag, New York.

Newton, R. C. & Perkins, D. III 1982. Thermodynamic calibration of geobarometers based on the assemblages garnet–plagioclase–orthopyroxene–(clinopyroxene)–quartz. *American Mineralogist*, **67,** 203–222.

Oliver, G. J. H., 1977. Feldspathic hornblende and garnet granulites and associated anorthosite pegmatites from Doubtful Sound, Fiordland, New Zealand. *Contributions to Mineralogy and Petrology*, **65,** 111–121.

Oliver, G. J. H., 1980. Geology of the granulite and amphibolite facies gneisses of Doubtful Sound, Fiordland, New Zealand. *New Zealand Journal of Geology and Geophysics*, **23,** 27–41.

Oliver, G. J. H., 1990. An exposed cross-section of continental crust, Doubtful Sound, Fiordland, New Zealand: geophysical and geological setting. In: *Exposed Cross-Sections of the Continental Crust: Proceedings. NATO ASI Series. Series C: Mathematical and Physical Sciences* (ed. Salisbury, M.H.), **317,** pp. 43–69.

Perchuk, L. L. & Lavrent'eva, I. V., 1990. Some equilibria involving garnet, orthopyroxene and amphibole as geothermometers and geobarometers for metamorphic rocks. In: *Experiment-89* (ed. Zharikov, V.A.), pp. 44–45. Izd. Nauka *Moscow, USSR*.

Powell, R., 1985. Regression diagnostics and robust regression in geothermometer geobarometer calibration – the garnet clinopyroxene geothermometer revisited. *Journal of Metamorphic Geology*, **3,** 231–243.

Rubatto, D. & Gebauer, D., 2000. Use of cathodoluminescence for U–Pb zircon dating by ion microprobe; some examples from the Western Alps. In: *Cathodoluminescence in Geosciences* (eds Pagel, M., Barbin, V., Blanc, P. & Ohnenstetter, D.), pp. 373–400.

Tulloch, A. J. & Kimbrough, D. L., 1989. The Paparoa metamorphic core complex, New Zealand; Cretaceous extension associated with fragmentation of the Pacific margin of Gondwana. *Tectonics*, **8,** 1217–1235.

Tulloch, A. J., Ireland, T. R., Walker, N. W. & Kimbrough, D. L., 2000. *U–Pb Zircon Ages from the Milford Orthogneiss, Milford Sound, Northern Fiordland: Paleozoic Igneous Emplacement and Early Cretaceous Metamorphism*. Science Report, 2000/6 . Institute of Geological and Nuclear Sciences.

Wandres, A. M., Weaver, S. D., Shelley, D. & Bradshaw, J. D., 1998. Change from calc-alkaline to adakitic magmatism recorded in the early Cretaceous Darran Complex, Fiordland, New Zealand. *New Zealand Journal of Geology and Geophysics*, **41,** 1–14.

Weaver, S. D., Bradshaw, J. D. & Adams, C. J., 1991. Granitoids of the Ford Ranges, Marie Byrd Land, Antarctica. In: *Geological Evolution of Antarctica; Proceedings of the Fifth International Symposium on Antarctic Earth Sciences* (eds Thomson, M.R.A., Crame, J.A. & Thomson, J.W.), pp. 345–351.

Weaver, S. D., Bradshaw, J. D. & Muir, R. J., 1994. Cretaceous magmatism in Marie Byrd Land and New Zealand; change from subduction to continental rifting. In: *Geological Society of New Zealand 1994 Annual Conference: Programme and Abstracts*. Geological Society of New Zealand, New Zealand, **80A,** 185 pp.

White, P. J., 1994. Thermobarometry of the Charleston metamorphic group and implications for the evolution of the Paparoa metamorphic core complex, New Zealand. *New Zealand Journal of Geology and Geophysics*, **37,** 201–209.

Williams, I. S. & Claesson, S., 1987. Isotopic evidence for the Precambrian provenance and Caledonian metamorphism of high grade paragneisses from the Seve Nappes, Scandinavian Caledonides: 2. Ion microprobe zircon U–Th–Pb. *Contributions to Mineralogy and Petrology*, **97/2,** 205–217.

Williams, J. G. & Harper, C. T., 1978. Age and status of the Mackay Intrusives in the Eglinton-Upper Hollyford area. *New Zealand Journal of Geology and Geophysics*, **21,** 733–742.

Williams, I. S., Chappell, B. W., Chen, Y. D. & Crook, K. A. W. 1992, Inherited and detrital zircons; vital clues to the granite protoliths and early igneous history of southeastern Australia. *Geological Society of America*, **272,** 503.

Wysoczanski, R. J., Gibson, G. M. & Ireland, T. R., 1997. Detrital zircon age patterns and provenance in late Paleozoic-early Mesozoic New Zealand terranes and development of the paleo-Pacific Gondwana margin. *Geology*, **25,** 939–942.

Received 12 May 2003; revision accepted 1 June 2004.